Investigation of Seismic Design of Slab-on-Girder Bridge Details in Alabama

by

Joseph Daniel Broderick

A thesis submitted to the Graduate Faculty of
Auburn University
in partial fulfillment of the
requirements for the Degree of
Master of Civil Engineering

Auburn, Alabama
August 5, 2018

Approved by

Justin D. Marshall, Ph.D., P.E., Chair, Associate Professor of Civil Engineering
J. Michael Stallings, Ph.D., P.E., Professor of Civil Engineering
Robert W. Barnes, Ph.D., P.E., Associate Professor of Civil Engineering

Abstract

The Alabama Department of Transportation (ALDOT) requested assistance to simplify and evaluate the process of designing typical slab-on-girder bridges for seismic loads. First, the determination of the seismic hazard in Alabama was made more expedient by providing hazard maps by each county within the state. Second, standard details were created to aid in the design of the plastic hinge zone within reinforced concrete columns. Third, the procedure for calculating the required support length at bents was studied. Next, the superstructure-to-substructure connection was investigated to determine whether adequate load path and capacity are provided to transfer seismic loads. Finally, the end diaphragms of steel girder bridges were designed for seismic loads to determine whether the current design methodology provides adequate resistance. It was determined that the superstructure-to-substructure connection did not provide adequate load path and anchor bolt strength, therefore improvements were recommended for future use in ALDOT's designs. The end diaphragms were determined to be adequate with the inclusion of seismic loads in design.

Acknowledgements

I would like to thank the Alabama Department of Transportation for their provision of construction drawings of steel girder bridges. They provided much needed information throughout this research process that aided in determining the recommendations made within this thesis.

I would like to thank Dr. Justin Marshall for his willingness to share his knowledge with me and to guide me through this research process. His humility, leadership, and encouragement were invaluable in bringing this thesis to completion and developing me as an engineer.

I would like to thank Hongyang Wu for his camaraderie and time during the two years we spent working on this project together. He, along with the civil engineering faculty and other graduate students, provided me with substantial support.

I would like to thank my beautiful and patient wife, Bethany, for her love and support throughout my career at Auburn University. Along with my daughter, Karis, the joy that they give me is immeasurable.

"Now to him who is able to keep you from stumbling and to present you blameless before the presence of his glory with great joy, to the only God, our Savior, through Jesus Christ our Lord, be glory, majesty, dominion, and authority, before all time and now and forever. Amen (Jude 1:24-25)."

Table of Contents

Abstract ii

Acknowledgements iii

List of Tables vii

List of Figures viii

Chapter 1: Introduction 1

1.1 Problem Statement 1

1.2 Problem Overview 1

1.3 Organization of Thesis 4

Chapter 2: Literature Review 5

2.1 Effects of Seismic Events on Bridges 5

2.1.1 Seismic Hazards and Analysis Method 5

2.1.2 Ductile Response and Energy Dissipation 7

2.1.3 Support Length 8

2.1.4 Load Path 10

2.1.5 End Diaphragms 12

2.2 Summary 13

Chapter 3: Seismic Hazard 14

3.1 Introduction 14

3.2 Hazard Determination 14

3.3 Hazard Maps 16

3.4 Summary 18

Chapter 4: Plastic Hinge Zone 19

4.1 Introduction 19

4.2 Plastic Hinge Zone Requirements 19

4.3 Plastic Hinge Zone Standard Drawings 21

4.4 Summary 23

Chapter 5: Support Length 24

5.1 Introduction 24
5.2 Definitions 24
5.3 Procedure 25
5.4 Results 28
5.5 Summary 29
Chapter 6: Superstructure-to-Substructure Connection for Steel Girder Bridges 30
6.1 Introduction 30
6.2 ALDOT's Connection and Load Path 31
6.3 Bridge Selection and Overview 33
6.4 Connection Design Validation 35
6.4.1 Seismic Hazard and Load Determination 35
6.4.2 Analytical Bridge Models 38
6.4.3 Elastomeric Bearing Models 41
6.4.4 Superstructure-to-Substructure Connection Design 43
6.5 Discussion 49
6.6 Recommendation 50
6.6.1 Shear Block Design Procedure 51
6.7 Summary 54
Chapter 7: End Diaphragm of Steel Girder Bridges 56
7.1 Introduction 56
7.2 ALDOT's End Diaphragms 57
7.3 End Diaphragm Model 59
7.4 End Diaphragm Design 60
7.5 Summary 64
Chapter 8: Summary, Conclusions, and Recommendations 66
8.1 Summary 66
8.2 Conclusions 67
8.3 Recommendations 68
8.4 Further Research 68

References....70
APPENDIX A: SAMPLE CALCULATIONS....72

List of Tables

Table 5.1: Support Lengths 28
Table 5.2: Displacement Limit and Maximum Span Displacements 29
Table 6.1: Seismic Hazard Values 36
Table 6.2: Equivalent Static Loads 37
Table 6.3: Simplified Uniform Loads 38
Table 6.4: Stiffness of Elastomeric Bearings 43
Table 6.5: Factored Connection Loads 44
Table 6.6: Connection Weld Capacities 45
Table 6.7: Anchor Bolt Bending Moments 47
Table 6.8: Flexural and Shear Capacities of Anchor Bolts 49
Table 6.9: Shear Block Design Details 54
Table 7.1: Diaphragm Members Demand and Capacity 64

List of Figures

Figure 3.1: Seismic Hazard Map for Site Classes A and B 16
Figure 3.2: Seismic Hazard Map for Site Class C 17
Figure 3.3: Seismic Hazard Map for Site Class D 17
Figure 3.4: Seismic Hazard Map for Site Class E 18
Figure 4.1: Plastic Hinge Zone Standard Drawings 22
Figure 5.1: Support Length and Displacement Limit Definitions 25
Figure 6.1: Superstructure-to-substructure connection (ALDOT, 2018) 32
Figure 6.2: Sole Plate Plan View (ALDOT, 2018) 33
Figure 6.3: Walker County Bridge Cross Section 40
Figure 6.4: Transverse Seismic Loads 41
Figure 6.5: Shear Block 52
Figure 7.1: Walker County End Diaphragm (ALDOT, 2018) 58
Figure 7.2: Limestone County End Diaphragm (ALDOT, 2018) 58
Figure 7.3: Montgomery County End Diaphragm (metric units) (ALDOT, 2018) 59
Figure 7.4: Walker County Diaphragm Axial Forces 60

Chapter 1: Introduction

1.1 Problem Statement

The state of Alabama has a seismic hazard that varies from a low hazard in the southern part of the state to a moderate hazard in the northern part of the state. Seismic design is a requirement for all bridges, and the difficulty of that design varies depending on the hazard level. Because Alabama has a low to moderate hazard, the Alabama Department of Transportation's (ALDOT) Bridge Bureau desires to simplify the seismic design process and make it as efficient as possible. One way to achieve this is by increasing familiarity with current design methods and making use of design aids and standard drawings. Previous research by Law (2013) investigated how to achieve this for details of prestressed concrete girder bridges whereas this thesis will mainly deal with steel girder bridges. This project will specifically investigate the details for the plastic hinge zone, the support length, the superstructure-to-substructure connection, and the end diaphragms. Because these details are focused on simplification, the studies conducted in this thesis only apply to "regular bridges" and not "critical bridges." The design for any bridge with a unique geometry, large span length, etc. will not be able to use these simplified processes.

1.2 Problem Overview

The majority of costs for construction of bridges has shifted towards labor costs and lane downtime rather than material costs. Because of this, construction policies have adopted standardized and simplified practices. These policies ultimately lead to

standardized and simplified design procedures as well. Determining the seismic hazard for any bridge is now achieved through contour maps provided by the American Association of State Highway and Transportation (AASHTO) Guide Specifications for Load and Resistance Factor Design (LRFD) Seismic Bridge Design (AASHTO, 2011). These contour maps are generally difficult to read with an adequate level of precision, thus, to contribute to efficiency and simplification of design, breaking down the seismic hazard of the state of Alabama by county is desired. The first topic covered will be the process that was used to develop simplified seismic hazard maps of Alabama.

The AASHTO LRFD Bridge Design Specifications identify an earthquake as an "Extreme Event" where "the structure may undergo considerable inelastic deformations" (LRFD, 2014). One design practice that has been adopted to ensure that these inelastic deformations do not cause failure or collapse of the bridge spans is to use a ductile fuse in the substructure in the form of a flexural plastic hinge. This hinge is a region within the reinforced concrete columns where special reinforcement detailing is provided to allow a ductile mechanism to form within the column during a seismic event. Several issues have arisen from the requirements of this plastic hinge zone, and the second topic of this report will address these problems and provide a standard drawing of the hinge zone for clarity.

Another event that may occur during a seismic event is the unseating of the bridge spans due to excessive span displacement from ground motions. Panzer (2013) investigated the potential for unseating in several Alabama bridges by running nonlinear dynamic analyses to determine the maximum span displacements. One of the ways to ensure that spans do not come unseated is to provide enough support length at the bents. Law (2013) investigated the results of several different equations to calculate the required

seat length. The third topic investigated in this thesis will be to combine the results of these two previous reports and make a recommendation on the requisite seat length to prevent unseating.

The fourth topic of this thesis is the connection between the superstructure and substructure. It is critical that a complete load path exists throughout the entire bridge structure and that each element within the structure is able to resist the loads that are applied to it. Although a seismic event is dynamic, the AASHTO Guide Specifications (2011) allow for a static analysis and load to be applied to the structure. Complete bridge models were created and analyzed to determine the effects on the superstructure-to-substructure connection. These effects were used in the design verification of the connection. Previous research by Law (2013) made recommendations for improvements to the connection in prestressed concrete girder bridges but these recommendations were declined by ALDOT because of their complexity for construction. Thus, an effort was made to validate the current connection that ALDOT uses for steel girder bridges and recommend necessary changes.

Large deformations are expected to occur during a seismic event, and steel girders tend to be susceptible to twisting under large deformations of the cross section. A key component in resisting this twist is the steel diaphragms located between the girders. The diaphragms that are most critical under lateral loads are those located at the supports. The goal for this thesis in reference to the diaphragms is similar to the connection between the superstructure and substructure—that is, analyzing the diaphragms, validating the current design that ALDOT uses, and making recommendations for needed modifications.

1.3 Organization of Thesis

Following this, Chapter 2 will discuss previous research in similar topics to this thesis that are useful in understanding the background of these topics. Chapter 3 will then discuss the procedure for determining the seismic hazard of a site and the steps that were taken to simplify this procedure. Chapter 4 will discuss the plastic hinge zone of reinforced concrete columns and provide the standard drawing for the required details. The support length that is required at each support will be investigated in Chapter 5. Subsequently, the connection between the superstructure and substructure will be studied in Chapter 6 to determine any recommendations that can be made. Then the diaphragms located at the bridge supports will be considered for their ability to resist seismic loads in Chapter 7. Finally, Chapter 8 will summarize this thesis as well as offer conclusions and recommendations that can be made from the topics studied.

Chapter 2: Literature Review

2.1 Effects of Seismic Events on Bridges

This chapter will study several aspects of slab-on-girder bridges and how they respond during a seismic event. The main damage to structures during a seismic event is caused by the ground motions that are propagated during the event. These ground motions are most powerful near the origin of the earthquake and reduce in intensity as they travel outward. Although the origin of the damage comes from the ground motions, there are no outside forces applied to the structure from the earthquake. All the forces generated by a seismic event are inertial forces caused by the structure resisting an acceleration. Because of the way that these forces are generated, they are highly dynamic and require specific design criteria in order for a structure to resist them (Chen & Duan, 2003).

2.1.1 Seismic Hazards and Analysis Method

Seismic hazard varies significantly throughout the United States, and a location's hazard is generally higher the closer it is to an active fault. Consequently, the AASHTO Guide Specifications have developed contour maps that define the hazard for the United States (AASHTO, 2011). There are multiple set of maps for each different soil condition that can be present because hazard of a specific construction site depends on the condition of the soil at the site. Depending on the soil profile at the abutment or bents, ground motions can be amplified or deamplified (AASHTO, 2011). The soil profile should be tested before the design of the structure and labeled as Site Class A through F,

with Site Class A (hard rock) amplifying ground motions the least and Site Class F (soils requiring site-specific evaluations) amplifying them the most. Even at sites containing the worst Site Class, the state of Alabama has a low to moderate seismic hazard, which enables the designer to use a simplified analysis as long as the bridge is not critical or essential (AASHTO, 2011).

AASHTO has identified different design methods to address the unique challenges that are associated with a seismic event. Based on the level of seismic hazard of the bridge's location and the importance of the structure, the method that is used for design may be a simplified static analysis, a more complex dynamic analysis, or a more complex time history analysis. The static analysis that AASHTO (2011) has adopted is called the Equivalent Static Analysis (ESA), which is "considered to be best suited for structures or individual frames with well-balanced spans and uniformly distributed stiffness where the response can be captured by a predominant translational mode of vibration."

The bridges that are studied within this thesis fit this description, and thus, the ESA is used for the analysis of this project. The specifications mention two types of ESAs—the uniform load method and the single-mode spectral analysis. The uniform load method uses equivalent static uniform loads that estimate the effects of seismic loads. This method is the simplest form of ESA, and thus will be used within this thesis. However, it is noted within the AASHTO Guide Specifications that this method can "overestimate the transverse shears at the abutments by up to 100 percent" (AASHTO, 2011). Clearly, the simplification of this analysis method is coupled with conservatism.

2.1.2 Ductile Response and Energy Dissipation

The AASHTO LRFD Specifications (2014) identifies an earthquake as an "Extreme Event" where "the structure may undergo considerable inelastic deformations" (LRFD, 2014). This presents the challenge of how to design the structure to undergo these deformations while taking minimal damage. One of the ways that engineers have attempted to do this is through energy dissipation by ductile deformation mechanisms. Because seismic events impart dynamic forces onto a structure, substantial amounts of energy are being applied throughout the structure (Chen & Duan, 2003). To try to minimize this, different methods of energy dissipation have been developed. While conventional bridges do not use any specific devices to achieve this, all structures have some inherent energy dissipation means within them. These include, but are not limited to, concrete cracking, steel yielding, and friction at joints (Chen & Duan, 2003). Obviously allowing too much energy dissipation through these means would not be ideal; thus, AASHTO Guide Specifications (2011) state that bridges should be designed for the superstructure to remain elastic while the substructure develops plastic deformations that result in these types of energy dissipation. This method of design has many benefits. First, the bridge can and should be designed in a way that will not result in ultimate collapse and will allow emergency vehicles to pass after a design event (AASHTO, 2011). Second, the substructure can be designed so that these means of energy dissipation (mainly concrete cracking and steel yielding) can be developed in specific zones of the column (Chen & Duan, 2003). These zones are referred to as plastic hinge zones and they have multiple requirements and benefits.

Bridges are not designed to allow the substructure to remain elastic during a seismic event because doing so would be uneconomical. The large inertia loads induced by the earthquake are too large to attempt to resist them elastically. Thus, plastic hinges are formed from these large forces within the concrete column. Engineers design the area that develops the plastic hinge to have high ductility in order to dissipate the energy that is imparted to the structure from the earthquake (Mander, 1983). Ductile elements are defined as "Parts of the structure that are expected to absorb energy and undergo significant inelastic deformations while maintaining their strength and stability" (AASHTO, 2011). To allow the plastic hinge zones to behave in a ductile fashion, there are special detailing requirements for the reinforcement within the zone. While the requirements mainly apply to the transverse reinforcement, some requirements are placed on the longitudinal reinforcement as well. Mander (1983) states "The ductility capacity of reinforced concrete members is achieved by providing sufficient transverse reinforcement in the form of rectangular hoops or spirals to adequately confine the concrete, to prevent buckling of longitudinal reinforcement, and to prevent shear failures." In short, the plastic hinge zones within the columns are critical to the overall behavior of the bridge during a seismic event.

2.1.3 Support Length

As previously stated, spans of bridges are expected to undergo significant displacement during an earthquake. Because of this, simply supported spans are vulnerable to becoming unseated from ground motions. If a span becomes unseated, then the bridge becomes impassable to all traffic, which is against the guidelines of design for bridge structures (AASHTO, 2011). To counter this, AASHTO Guide Specifications

(2011) require a minimum amount of seat length to be provided. The Applied Technology Council and Multidisciplinary Center for Earthquake Engineering Research performed research during a Joint Venture (2003) on the calculation of minimum support length. They state, "The requirement for minimum seat width accounts for (1) relative displacement due to out-of-phase ground motion of the piers, (2) rotation of pier footings, and (3) longitudinal and transverse deformation of the pier" (ATC/MCEER, 2003). They determined that the AASHTO Standard Specification underestimate the longitudinal and transverse deformation of the columns and recommended an alternate equation for calculating the support length. Their equation scales the support length directly to the seismic hazard whereas the AASHTO equation provides a flat multiplier based on the Seismic Design Category (ATC/MCEER, 2003). Providing enough support length is essential for preventing the unseating of bridge spans.

Previous research by Law (2013) further investigated the difference between the AASHTO equation for support length and the ATC/MCEER equation. A case study of five bridges was conducted to determine what requisite support length each bent of each bridge would give for each equation. Law (2013) concluded that the ATC/MCEER equation gave results that were more conservative in areas of moderate seismic hazard. Panzer (2013) also conducted analyses of the same five bridges which focused on determining the span displacements. Nonlinear time-history analyses were conducted of each bridge with several different ground motions to determine the displacement of each span of the bridges (Panzer, 2013). The goal was to determine if any spans were in danger of becoming unseated based on the span displacements and provided support length.

The main reason for investigation of this topic is that ALDOT declined the recommendation that Law (2013) made for improvement of their superstructure-to-substructure connection. Thus, their connection still contains no positive load resistance in the longitudinal direction—only the friction between the bearing pad and the girder provides any resistance. Thus, the support length must be sufficient to allow the superstructure to withstand ground motions without becoming unseated.

2.1.4 Load Path

Another essential aspect of bridges is the ability to transfer loads between the superstructure and substructure. Historically, this has been done through connection at the beam support. ALDOT's standard is using an elastomeric bearing pad to provide this connection. These pads consist of alternating layers of elastomer and steel reinforcing shims that together make up a mechanical system that will "allow the translation and rotation of a bridge while carrying its gravity load to the substructure and foundation" (Konstantinidis, Kelly, & Makris, 2008). Konstantinidis et al. (2008) studied the effects of three different types of bearings under seismic loads: elastomeric bearings, PTFE-elastomeric bearings, and spherical bearings. Regular elastomeric bearings consisted of just the bearing pad itself resting between the girder and the bent cap. PTFE-elastomeric bearings consisted of the bearing pad inserted between two steel end plates with a polytetrafluoroethylene (PTFE) sliding surface on top of the assembly. The spherical bearing consisted of a steel convex plate covered in a PTFE surface with a concave plate resting on top (Konstantinidis et al., 2008). Of these three bearings tested, the PTFE-elastomeric bearing is the closest to the bearing studied in this thesis.

Typically, these bearings are only designed for thermal expansion and to allow the superstructure to move and rotate relative to the substructure. However, to determine their behavior during seismic loads, Konstantinidis et al. (2008) placed an assembly of the bearing, superstructure, and substructure under cyclic loading. The general idea behind the PTFE bearing is that the bearing pad will allow for rotations of the superstructure while the sliding surface of the PTFE will allow for translation. However, the first finding during this study was that the steel plates on top of the bearing pad prevented any real rotation from occurring without immediate damage to the plates. Second, the cyclic loading caused large amounts of damage to the PTFE surface. Konstantinidis et al. (2008) stated that it was not clear if this damage affected the performance of the surface or the assembly, but it does require maintenance after a seismic event does occur to ensure the full capabilities of the bearing are available.

In general, one of the main benefits of bearing pad assemblies is they allow a reliable transfer of forces with little maintenance (Konstantinidis et al., 2008). More benefits of the bearing assemblies consist of efficiency in terms of economy and longevity of life (Yazdani, Eddy, & Chun, 2000). Despite the many benefits and the importance of the bearing pads in transferring the forces from the superstructure to the substructure, the design of these assemblies is often incomplete and neglected (Mander, Kim, Chen, & Premus, 1996). The California Department of Transportation created a design memorandum to bridge design engineers about the design of the bearing assemblies and stated, “Too often bearings are selected at the last minute when forces and available space are fixed” (Caltrans, 1994). Although the state of Alabama has a

relatively low seismic hazard, effort should still be placed in the design of these bearings to ensure that the benefits of their low maintenance and longevity are maximized.

2.1.5 End Diaphragms

Another aspect of steel girder bridges that is associated with the movement of the superstructure are diaphragms, or cross-frames. Rather than controlling the rotation or translation of the superstructure, diaphragms prevent the twisting of the girder cross sections (Helwig & Wang, 2003). Diaphragms typically contain truss elements spanning between the girders with a top and bottom chord near the top and bottom flange of the girders while braces connect the respective chords together. This configuration allows the truss elements to resist the twisting of the girder through axial resistance. By resisting the twisting of the girders, the capacity of the girders is increased because the girder unbraced length is shortened and lateral-torsional buckling of the girder is constrained (Helwig & Wang, 2003).

Historically, ALDOT has not designed diaphragms for seismic loading. However, diaphragms at the supports (referred to here as “end diaphragms”) can have large internal forces produced due to lateral loads (Zahrai & Bruneau, 1998). Moreover, AASHTO Guide Specifications (2011) require that diaphragms be designed for lateral loads and even specifies that they should be considered main force resisting members in skewed or curved bridges. In fact, end diaphragms are so significant that research has been conducted to retrofit bridges with ductile diaphragms to take the place of a ductile substructure. Zahrai and Bruneau (1998) conducted analytical studies to determine the effectiveness of ductile end diaphragms for seismic retrofit. The goal of the ductile end diaphragms is to design them to yield before the substructure has undergone plastic

deformations, thereby eliminating the need for the difficult repair of the reinforced concrete columns. Zahrai and Bruneau (1998) found that, “It is possible, in some instances, to seismically retrofit slab-on-girder steel bridges by replacing their existing end-diaphragms with new ductile diaphragms.” Their study consisted of stiff substructures instead of flexible substructures which required them to recommend more research before the system could be implemented. While the seismic hazard in Alabama is likely not high enough to require this level of detailing, this research points to the significance that end diaphragms can play under lateral loads.

2.2 Summary

This chapter provided an overview of the effects of seismic events on bridges. Several key aspects of the behavior of bridges under seismic loads were introduced and studied. Seismic design can be complicated for engineers who do not study or design for it regularly to fully understand, which makes simplified design aids valuable. Understanding how each element of a slab-on-girder bridge behaves during ground motions is critical to ensuring efficient implementation of design and construction. Familiarization with the seismic response of bridges also aids in designs being capable of survival and limited functionality. The aspects that were studied here will be further discussed and studied in the following chapters.

Chapter 3: Seismic Hazard

3.1 Introduction

The first step in seismic design of structures is to determine the seismic hazard of the site. This is currently accomplished by using contour maps within AASHTO Guide Specifications (2011) or by using an online tool on the USGS website to determine the Seismic Design Category (SDC). However, in order to streamline the design process, maps of Alabama were created that delineated the SDC by each county. By creating visual maps, the designer can more quickly determine whether any seismic detailing is needed. Seismic detailing is needed in any location that has a one-second design spectral acceleration (S_{D1}) of 0.10g or more (AASHTO, 2011). While this procedure will simplify the approach to determining the hazard, conservatism is built in to the procedure, and thus it may provide a seismic hazard that is more stringent than if a more precise procedure was followed.

3.2 Hazard Determination

The first step in determining the seismic hazard for Alabama is determining the Site Class of the construction site. There are multiple ways to determine the soil conditions at a site, with the most common way being to conduct a Standard Penetration Test (SPT) to count the number of blows (N_i) required to penetrate a layer of soil, and the most accurate way being to conduct a Shear Wave Velocity Test. The SPT is a simplified way to estimate the shear wave velocity of a soil. After this test is completed, Equation 3.1 is used to calculate the average standard penetration blow count (N). Based on this

value and Table 3.4.2.1-1 in the AASHTO Guide Specifications (2011), the Site Class is determined. One limitation of this test is that it can only be applicable to Site Classes C-F. To be able to use the seismic hazard in a Site Class of A or B, the Shear Wave Velocity test must be used. One note to make is that although the Site Classes can be identified all the way to Site Class F, Site Class F is uncommon and must be specifically tested which resulted in a hazard map not being developed for this Site Class.

$$N = \frac{\sum_{i=1}^{n} d_i}{\sum_{i=1}^{n} \frac{d_i}{N_i}} \qquad \text{Equation 3.1}$$

Where N = Average standard penetration blow count
n = total number of distinctive soil layers in the upper 100 ft of the site profile
i = any one of the layers between 1 and n
d_i = thickness of *i*th soil layer
N_i = Uncorrected blow count of *i*th soil layer

After determining the site class, the United States Geological Survey (USGS) seismic hazard batch-mode tool can be used to determine multiple variables that will be used to determine the SDC. To create the seismic hazard maps, the USGS tool was used to obtain the hazard at six different locations in each county around the perimeter of the county (USGS, 2018). Google maps were used to find the coordinates of these six locations, and the coordinates were input into the USGS tool (Google, 2018). The tool outputs numerous variables, but the most important variables obtained were the peak ground acceleration (A_s), the short period design (0.2 s) spectral acceleration (S_{DS}), the one second design spectral acceleration (S_{D1}), and the SDC. The values for every point and every county were listed in an accessible database for future design. Each county was labeled based on the worst case SDC from the six coordinates. An online tool provided by mapchart.net was used to create the maps (mapchart, 2018).

3.3 Hazard Maps

The hazard maps are presented below in Figures 3.1-3.5. It is clear from the maps that as the Site Class is increased, the SDC is also increased. Another pattern that is clear is the more northern or western the location, the higher the hazard. This pattern originates from the fact that the New Madrid seismic zone is located to the north-west of Alabama and the East Tennessee Seismic Zone is located to the north-east of the state.

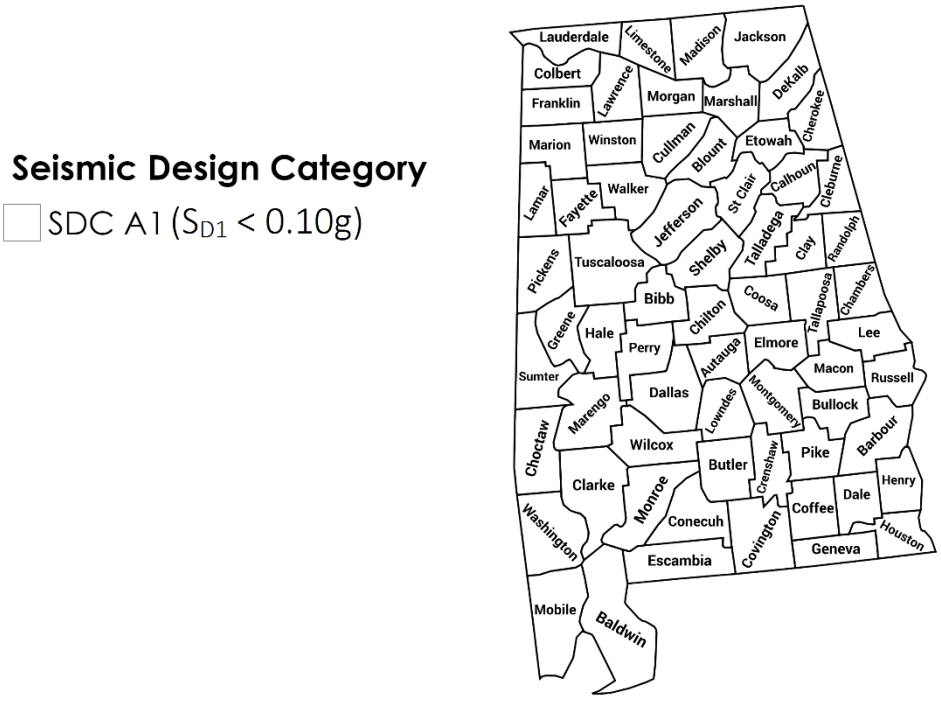

Figure 3.1: Seismic Hazard Map for Site Classes A and B

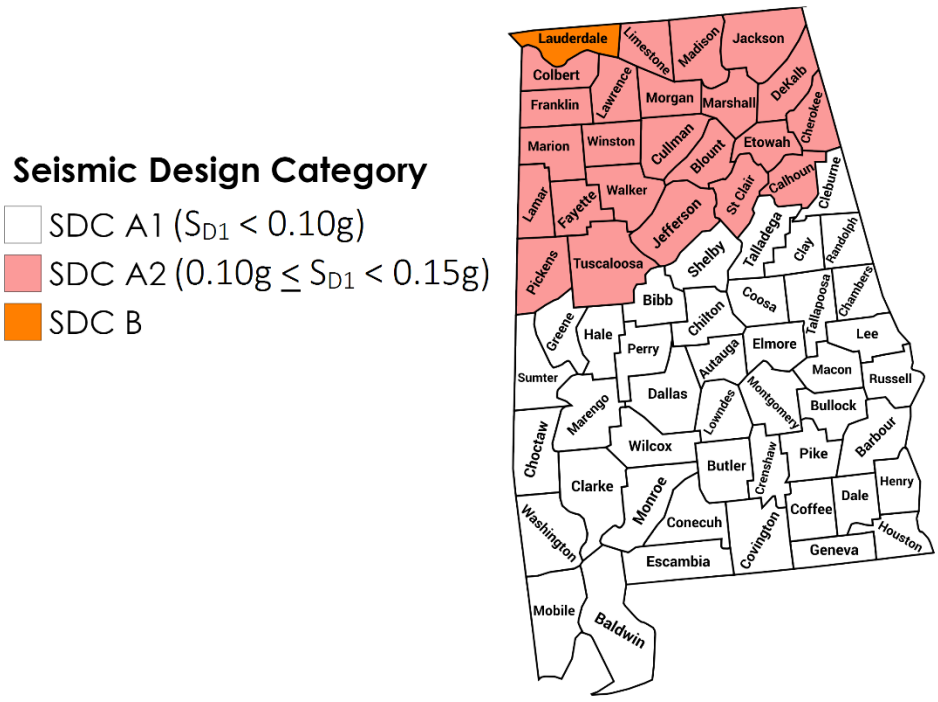

Figure 3.2: Seismic Hazard Map for Site Class C

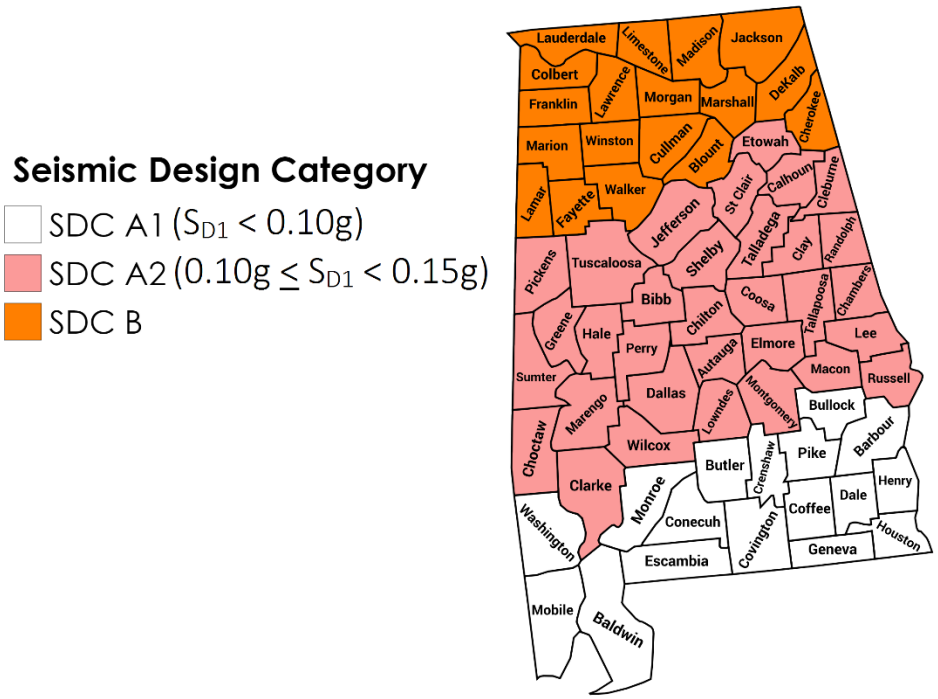

Figure 3.3: Seismic Hazard Map for Site Class D

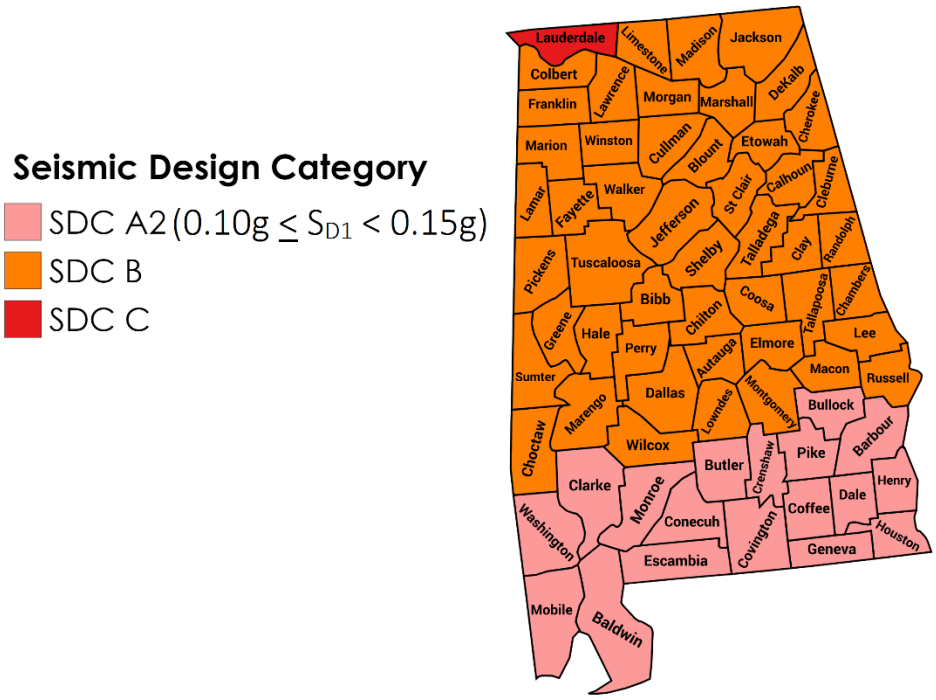

Figure 3.4: Seismic Hazard Map for Site Class E

3.4 Summary

This chapter established the procedure for determining the seismic hazard for a specific site and developed simplified hazard maps for each county and Site Class in Alabama. Engineers can use these maps and the ground motion values associated with each county to make their design process more expedient. Because this procedure is simplified, there is a certain amount of conservatism built in with it. The designer must balance the project's need for simplicity with its need for accuracy.

Chapter 4: Plastic Hinge Zone

4.1 Introduction

Bridges are not designed to allow the substructure to remain elastic during a design level seismic event because doing so would be uneconomical. The large inertial loads induced by the earthquake are too large to attempt to resist them elastically. Thus, plastic hinges are formed from these large forces within the concrete column. Engineers design the area that develops the plastic hinge to have high ductility in order to dissipate the energy that is imparted to the structure from the earthquake (Mander, 1983). Ductile elements are defined as, "Parts of the structure that are expected to absorb energy and undergo significant inelastic deformations while maintaining their strength and stability" (AASHTO, 2011). To allow the plastic hinge zones to behave in a ductile fashion, there are special detailing requirements for the reinforcement within the zone. While the requirements mainly apply to the transverse reinforcement, some requirements are placed on the longitudinal reinforcement as well. This chapter will discuss the requirements of the plastic hinge zone and will present a set of standard drawings in order to concisely display the requirements in the plastic hinge zone.

4.2 Plastic Hinge Zone Requirements

The first requirement for the plastic hinge zone is the length of the hinge zone. AASHTO Guide Specifications (2011) indicate that the length of the zone is the largest of:

- 1.5 times the largest column cross-sectional dimension

- The region of the column where the moment demand exceeds 75% of the maximum moment
- The analytical plastic hinge length, L_p

The analytical plastic hinge length is defined in AASHTO Guide Specifications (2011) 4.11.6 as Equation 4.1 below.

$$L_p = 0.08 * L + 0.15 * f_{ye} * d_{bl} \geq 0.3 * f_{ye} * d_{bl} \qquad \text{Equation 4.1}$$

Where L_p = Analytical plastic hinge length (in.)
L = Height of column (must be in.)
f_{ye} = Yield stress of longitudinal reinforcement (must be ksi)
d_{bl} = Diameter of longitudinal reinforcement (must be in.)

The next requirement for the plastic hinge zone is that longitudinal bars cannot be spliced within the zone. While this is only a requirement for SDC C and D, the commentary of the specifications recommend applying this to SDC B as well (AASHTO, 2011). One result from this requirement is that if a column has an aspect ratio (ratio of length to width) of less than 3.0, it can be difficult to have an area long enough within the column to splice the reinforcement. Thus, it is recommended that a minimum aspect ratio of 4.0 be used.

There are several requirements for the transverse reinforcement within the plastic hinge zone. First, the maximum spacing of transverse reinforcement in the zone is the smallest of:

- 1/5 the smallest dimension of the column cross-section
- 6 times the diameter of the longitudinal reinforcement
- 6 inches

If number 9 or smaller longitudinal reinforcement is used, the transverse reinforcement must be number 4 bars. If the longitudinal reinforcement is larger than number 9, the

transverse reinforcement must be number 5 bars. There are also minimum reinforcement ratios (ρ_t) depending on if the transverse reinforcement is spiral or rectangular. If it is spiral reinforcement, ρ_t must be at least 0.003 in SDC B or 0.005 in SDCs C and D. If the transverse reinforcement is rectangular, ρ_t must be at least 0.002 in SDC B or 0.004 in SDCs C and D. The transverse reinforcement also must be fully enclosed and developed in order to provide shear strength and confining pressure to the core concrete in the plastic hinge zone (AASHTO, 2011).

There is also a requirement for the plastic hinge zone to be extended into the bent cap or foundation for a certain length. This extends the plastic hinge zone spacing of transverse reinforcement into the foundation and cap beam. This extension ensures that strain penetration into the connecting elements is accounted for and that the transverse reinforcement will not fail in their anchorage. This extension is only required for SDCs C and D, but the commentary recommends applying it to SDC B as well. The extension is required to be the largest of (AASHTO, 2011):

- One-half the maximum column dimension
- 15 inches

4.3 Plastic Hinge Zone Standard Drawings

Based on the above requirements, a set of standard drawings was developed to illustrate the requirements in a concise manner. These drawings were developed in Autodesk Revit 2018 and a reduced version is shown below (Autodesk, 2018). The full version is presented on an 11x17 drawing sheet.

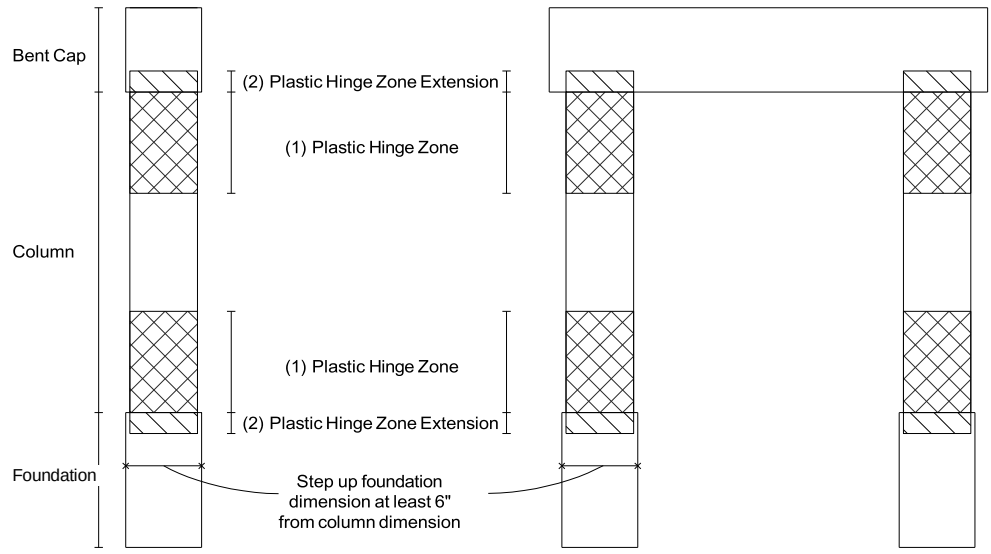

(1) Plastic Hinge Zone: *
- (A) Plastic Hinge Length largest of:
  - (i) 1.5 times largest column cross-sectional dimension
  - (ii) Region of column where the moment demand exceeds 75% of the maximum plastic moment
  - (iii) $L_P = 0.08*L + 0.15*f_{ye}*d_{bl} >= 0.3*f_{ye}*d_{bl}$
- (B) Cannot splice longitudinal bars within Plastic Hinge Zone (For SDC C and D) **
- (C) Maximum spacing of transverse reinforcement in Plastic Hinge Zone is least of:
  - (i) 1/5 the least dimension of the column cross-section
  - (ii) $6*d_{bl}$
  - (iii) 6 inches
- (D) #4 transverse reinforcement required if longitudinal reinforcement is #9 or smaller; #5 transverse reinforcement required otherwise
- (E) p_t must be at least 0.003 for spiral reinforcement in SDC B or 0.005 in SDCs C and D and 0.002 for rectangular reinforcement in SDC B or 0.004 in SDCs C and D

(2) Plastic Hinge Zone Extension:
- (A) Continue the Plastic Hinge Zone spacing of transverse reinforcement into the foundation and cap beam (For SDC C and D) **
- (B) Extension dimension largest of:
  - (i) 1/2 largest column dimension
  - (ii) 15 inches

* If S_{D1} is less than 0.10g, columns do not need to meet these requirements

** Requirements are only for SDC C and D; however, specification commentary recommends applying these requirements to SDC B as well

L = Column length (must be in.)

f_{ye} = Yield stress of longitudinal bars (must be ksi) d_{bl} = Diameter of longitudinal bars (must be in.)

p_t = Transverse reinforcement ratio

S_{D1} = One-Second Period Design Spectral Acceleration

Figure 4.1: Plastic Hinge Zone Standard Drawings

4.4 Summary

This chapter discussed the method that slab-on-girder bridges use to dissipate seismic energy—a ductile plastic hinge within the substructure. Standard drawings were created to aid in the design of the plastic hinge zone within the reinforced concrete columns. The plastic hinge zone has multiple requirements that must be met in order to ensure that a ductile response is established within the superstructure. A ductile response will allow the bridge to avoid collapse and remain open for emergency vehicles after a seismic event. Thus, accuracy and attention to detail when designing the plastic hinge zone is paramount.

Chapter 5: Support Length

5.1 Introduction

During a seismic event, there can be large amounts of movement for a bridge span, which makes it necessary to design for certain limit states. One of these limit states is the unseating of bridge spans, therefore determining how much support length is required at each support is necessary. Providing enough support length will ensure that the bridge spans can "ride out" a seismic event without becoming unseated. This is especially important for the current method of design in Alabama because there is no longitudinal restraint of the bridge spans, thus, they are at risk of becoming unseated due to ground motions. The purpose of this chapter is to determine which procedure to calculate the support length is recommended.

5.2 Definitions

AASHTO Guide Specifications (2011) define the support length, N, as "the length of overlap between the girder and the seat." Figure 5.1 gives a visual representation of what the support length is. In this chapter, a displacement limit will be placed on bridge spans that is assumed to be the limit state at which a bridge span will be at risk of becoming unseated. Unseating of a bridge span happens when the girders fall off the edge of the support and the span collapses. The displacement that is assumed to cause this is when the location of the girders that is aligned with the centerline of the bearing connection is displaced to the edge of the bent cap. This displacement limit is shown in Figure 5.1. This is a more conservative assumption than allowing the girder to

displace the full support length. This limit was chosen because it was assumed that the demand placed on the girders and bearing pad after this limit is reached may become too large.

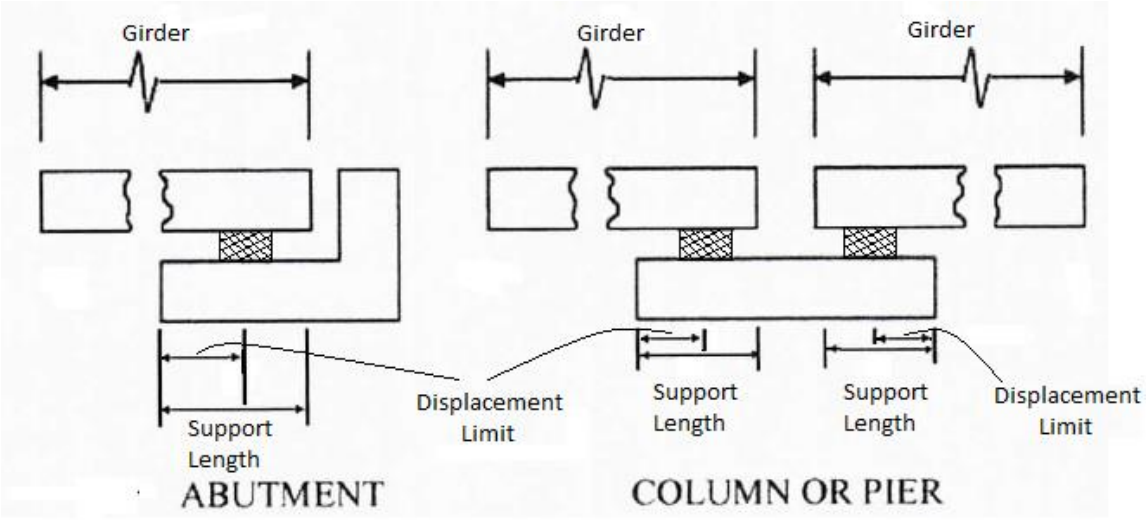

Figure 5.1: Support Length and Displacement Limit Definitions

5.3 Procedure

Two methods were used to calculate the required support length. The first method was the equation given by AASHTO Guide Specifications (2011) Article 4.12.2 in Equation 5.1. This equation is a function of the span length (L), the column height (H), and the angle of skew (S). This equation is only applicable to SDCs A, B, and C while SDC D has its own equation which is not investigated in this thesis. This equation is then increased by a percentage based on the SDC. For SDC B, it is increased by 150%.

$$N = (8 + 0.02L + 0.08H)(1 + 0.000125S^2) \qquad \text{Equation 5.1}$$

Where N = Support length (must be in.)
L = Span length (must be ft.)

H = Column height (must be ft.)
S = Angle of skew (must be degrees)

The Applied Technology Council (ATC) and the Multidisciplinary Center for Earthquake Engineering Research (MCEER) proposed the second method that was used (ATC/MCEER, 2003). Equation 5.2 was developed by the ATC/MCEER Joint Venture in 2003 and differed from the above AASHTO equation by including the S_{D1} coefficient in the calculation instead of multiplying the equation by a flat percentage. This allowed the support length calculation to be tailored to the seismic demand of the site.

$$N = \left(4 + 0.02L + 0.08H + 1.09\sqrt{H}\sqrt{1 + \left(2\frac{B}{L}\right)^2}\right) * \left(\frac{1+1.25S_{D1}}{\cos\propto}\right) \qquad \text{Equation 5.2}$$

Where B = Width of superstructure
S_{D1} = One second period design spectral acceleration
α = Angle of skew

Because of this, Law (2013) recommended to ALDOT that they use this equation instead of the AASHTO equation and use the highest S_{D1} that SDC B can have of 0.30g. By using this equation and this value of S_{D1}, the ATC/MCEER equation was more conservative than the AASHTO equation, but ALDOT decided that they did not want to use an equation that was not in the specifications. Law (2013) also suggested an improvement to the superstructure-to-substructure connection that would apply a positive load resistance mechanism in the longitudinal direction because ALDOT's connection provided no longitudinal resistance other than the friction between the bearing pad and the girder. ALDOT also declined to use this recommendation and instead wanted only to provide sufficient seat length to allow the superstructure to withstand any ground motions in the longitudinal direction. Thus, the goal of this chapter is to discover whether the span displacements analyzed by Panzer (2013) exceeded the support length capacity calculated

with Equation 5.1, or if this equation is adequate in determining the support length for the state of Alabama.

Three concrete girder bridges were used to investigate whether Equation 5.1 is adequate. These bridges will be labeled as Little Bear Creek bridge, Oseligee Creek bridge, and Scarham Creek bridge. Law (2013) and Panzer (2013) investigated different aspects of the support length for all three bridges previously. Law (2013) investigated the differences between methods of calculating the support length while Panzer (2013) investigated the presence of span unseating during different ground motions. It is important to note that the investigations completed by these theses were only conducted on prestressed concrete girder bridges with simple spans. These findings may not be directly transferrable to steel girder bridges with continuous spans.

Law's (2013) calculations of the support length using both equations were recorded for all bents of each bridge, then the structural drawings of these bridges were used to determine the actual provided seat length. Panzer (2013) ran several different analyses for each bridge while changing four main parameters for each analysis. The first analysis was run with a lower limit friction coefficient for the bearing pads of 0.20. The second analysis was run with an upper limit friction coefficient of 0.40. The next two analyses were with the same differing friction coefficients but with an MCE-level ground motion instead of a design ground motion. Span displacements were calculated from each of these analyses for each bridge, and these values were recorded from Panzer's (2013) thesis. The structural drawings of each bridge were then used to determine the displacement limit as defined in Section 5.2.

5.4 Results

Table 5.1 shows the calculated support length from both equations and the actual provided seat length from the construction drawings. In all cases except for Oseligee Creek bent 2, the provided support length was greater than or equal to the required support length calculated from Equation 5.1. In all cases except for Oseligee Creek bents 2 and 3, the provided support length was greater than or equal to the required support length calculated from Equation 5.2.

Table 5.1: Support Lengths

	Little Bear Creek Bent 2	Little Bear Creek Bent 3	Oseligee Creek Bent 2	Oseligee Creek Bent 3	Scarham Creek Bent 2	Scarham Creek Bent 3	Scarham Creek Bent 4
Equation 5.1 (in.)	17.3	17.9	16.5	17.5	20.0	23.0	19.8
Equation 5.2 (in.)	16.6	18.3	17.6	20.1	23.1	29.1	22.6
Provided Support Length (in.)	22.5	22.5	16.5	16.5	27.0	33.0	27.0

Although Table 5.1 may seem to show that Equation 5.1 is adequate for most cases, the values that need to be compared to determine if that is true are the displacement limit values. Table 5.2 shows the displacement limit and the maximum span displacements. The displacement limit exceeds the maximum span displacements in all cases. Because the displacement limit is greater than the maximum span displacements that Panzer (2013) calculated, Equation 5.1 is adequate in calculating the required support length.

Table 5.2: Displacement Limit and Maximum Span Displacements

		Max Span Displacements (in.)			
	Displacement Limit (in.)	Lower limit friction	Upper limit friction	MCE Lower limit friction	MCE Upper limit friction
Little Bear Creek Bent 2	10.5	2.35	2.75	3.05	2.85
Little Bear Creek Bent 3	10.5	2.35	2.75	3.05	2.85
Oseligee Creek Bent 2	9.00	3.28	3.21	4.44	4.77
Oseligee Creek Bent 3	9.00	3.28	3.21	4.44	4.77
Scarham Creek Bent 2	15.0	3.68	3.95	3.82	3.81
Scarham Creek Bent 3	21.0	3.68	3.95	3.82	3.81

5.5 Summary

The goal of this chapter was to determine whether the AASHTO Guide Specification's method of calculating the required support length is sufficiently conservative to provide enough support length with only friction due to gravity loads resisting any longitudinal ground motions. After comparing not only the provided support length to the required support length, but also the displacement limit to the calculated maximum span displacements, it was determined that Equation 5.1 provides sufficient support length. Therefore, it is recommended that ALDOT use the specification equation to determine the required support length, which will provide sufficient safety against span unseating without changing the connection configuration. It is important to note, however, that the research conducted by Law (2013) and Panzer (2013) was limited to prestressed concrete girders with simply supported spans. These findings may not be directly transferrable to steel girder bridges with continuous spans, although the only support length that is important in a continuous-span-steel-girder bridge are those at the abutments. Unseating is not possible for continuous spans without significant damage occurring before the unseating occurs.

Chapter 6: Superstructure-to-Substructure Connection for Steel Girder Bridges

6.1 Introduction

Alabama's most common type of bridge is the slab-on-girder bridge configuration which makes up a system that is split into two main components, the superstructure and the substructure. The superstructure consists of the deck, the roadway, and the girders, while the substructure consists of a reinforced concrete beam (referred to here as a "bent cap") that the girders rest on, columns that support the bent cap, and finally, the foundation which connects to the columns and completes the load path into the ground. One critical part of this system is the connection between the superstructure and the substructure. This chapter will investigate the connection between the superstructure and substructure of slab-on-girder steel bridges to determine whether the current connection that ALDOT uses is adequate in terms of load path and strength. A complete load path between the superstructure and substructure is critical to enable the ductile substructure to be effective. Thus, every part of the connection must be able to resist the lateral loads in each direction and transfer them to the ductile substructure.

Previous research by Law (2013) investigated the connection for prestressed girder bridges but this thesis will specifically look at the bearing connections for steel girder bridges. This thesis will investigate whether the superstructure-to-substructure connection provides an adequate load path for the structure and whether it provides adequate strength to resist Alabama's moderate seismic loads. If any improvements can

be made to the current connection detail, they will be recommended for ALDOT's future use. This chapter will provide details on the procedure taken to design the connection.

6.2 ALDOT's Connection and Load Path

ALDOT uses elastomeric bearing pads for this connection which "are designed to support the vertical compressive loads from bridge beams and to allow horizontal movement of beams due to thermal expansion and contraction, traffic loads, elastic shortening, beam end rotations, and time-dependent changes in concrete" (Yazdani, Eddy, & Cai, 2000, p. 224). A varying number of layers of neoprene and steel shims are alternated to form the elastomeric bearing pad connection that allows relative movement between the top and bottom of the pad (Yazdani et al., 2000). ALDOT's current bearing connection consists of four main components: the elastomeric bearing pad, a bearing plate fixed to the top of the bearing pad, a sole plate resting on the bearing plate, and anchor bolts connecting the sole plate to the bent cap. This connection is shown in Figure 6.1, and a plan view of the sole plate is shown in Figure 6.2.

The purpose of the bearing pad is explained above. The purpose of the bearing plate is to provide a sliding surface for the sole plate to slide along. The purpose of the sole plate is to both connect to the steel girder through welds and to connect to the bent cap through the anchor bolts. This system allows for a complete load path in the transverse direction (left and right in Figure 6.1) between the superstructure and the substructure. Shear force is transferred from the girders to the sole plate through welds and to the bent cap through the sole plate and anchor bolts. Although the load path is complete for the transverse direction, observation of the sole plate shows that because of the long-slotted holes, there is no complete load path in the longitudinal direction (in and

out of the page on Figure 6.1). The girders are free to slide in the longitudinal direction, so it is necessary to provide enough support length to allow the spans to “ride out” the ground motion without becoming unseated. This was discussed in further detail in Chapter 5 of this thesis. While this sole plate configuration is most common for the internal supports, ALDOT does sometimes provide a different configuration at the abutments that does not have long-slotted holes. While this connection would provide some longitudinal restraint, it was assumed that this restraint would not have adequate strength to resist the movement of continuous span steel girder bridges. This assumption will be confirmed with the study done in this chapter.

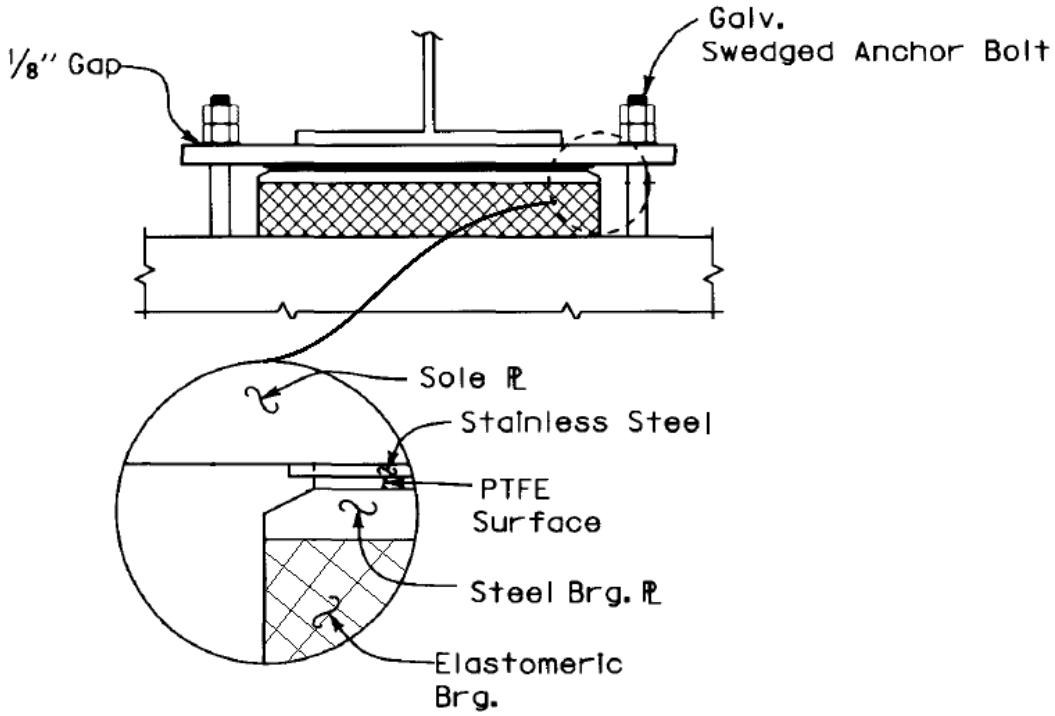

Figure 6.1: Superstructure-to-substructure connection (ALDOT, 2018)

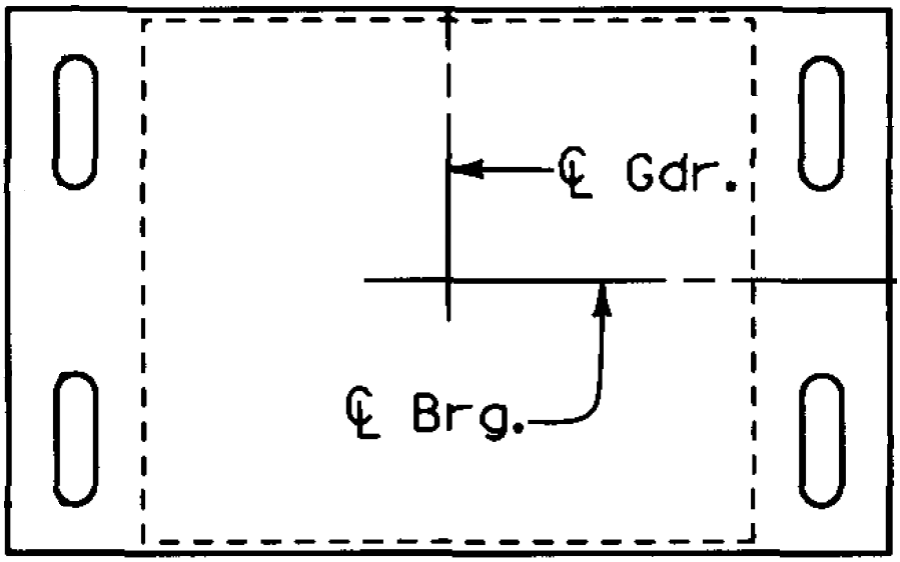

Figure 6.2: Sole Plate Plan View (ALDOT, 2018)

6.3 Bridge Selection and Overview

The three bridges that were analyzed were from Walker County, Limestone County, and Montgomery County. Limestone County is at the very northern edge of Alabama, Walker County is north central, and Montgomery is in central Alabama. This selection of bridges allowed for the analysis to represent a good sample of the seismic hazard in Alabama. The Walker County bridge consisted of four continuous steel girder spans and one simply supported prestressed girder span ranging between a 100-foot length and a 210-foot length for an overall length of 862 feet. The first four spans contained six steel girders with 8.5-foot web depths while the last span consisted of six Type BT-72 prestressed concrete girders. The construction project consisted of two bridges—one westbound bridge and one eastbound. The two bridges were nearly identical, only varying in small details such as elevations, and thus only one was considered for design in this thesis. The deck was a constant 58.75-foot width and 7.5-inch thickness. Each bent contained three circular columns ranging in height from 40 feet

to 90 feet and in diameter from 5 feet to 7.5 feet. Each bent used between one to two struts and either drilled shafts, spread footings, or battered pile foundations. While the prestressed girder span was included in the analytical model described below, the bearing connections between the prestressed girders and substructure were not considered for design.

The Limestone County bridge consisted of three continuous spans with two equal spans of 71 feet and one span of 158 feet for an overall length of 300 feet. The three spans contained eight steel girders with 5-foot web depths. The deck was a constant 56.75-foot width and 6.5-inch thickness. Each bent contained three circular columns with heights around 21 feet, diameters of 3.25 feet, and battered pile foundations.

The Montgomery County bridge consisted of nine spans with six prestressed concrete girder simple span lengths of 113 feet and three 200-foot steel girder continuous spans for an overall length of 1,275 feet. The prestressed girder spans contained five Type BT-1830 girders while the last three spans contained five steel girders with 7-foot web depths. The deck was a constant 42-foot width and 7.0-inch thickness. Each bent contained a single oval column that ranged from 12 feet by 5 feet to 15 feet by 6 feet with heights ranging from 50 feet to 65 feet. The bents used battered piles as their foundation. This bridge also contained a horizontal curve that started with the first steel girder span. The radius of the horizontal curve was 1000 feet and ended at the end abutment. Because this bridge had a horizontal curve, the Equivalent Static Analysis method that was described in Chapter 2 does not fit well as an analysis method for this bridge. However, this method was still used because ALDOT places great importance on the simplification of analyses. Precaution should be taken if the ESA method is used in the design of an

actual curved bridge and measures should be taken to address the inaccuracies of the model.

6.4 Connection Design Validation

The construction drawings of three steel girder bridges were provided by ALDOT for the investigation of the superstructure-to-substructure connection design. The first step taken was to determine the seismic hazard of each of the bridges in order to determine the loads that were applied. Analytical models were created for all three bridges using CSiBridge 15, which is a structural analysis and design program specifically for modeling bridge structures (Computer and Structures Inc., 2012). Special attention was placed on the method for modeling the superstructure-to-substructure connection which will be discussed in Section 6.4.3. After the models were complete, the structural analysis was run to determine the forces in each element. Finally, the strength of the connection was determined and compared to the demand. The following sections will detail each of these steps.

6.4.1 Seismic Hazard and Load Determination

In order to determine the demand on each element in the structure, the seismic hazard for each site must be determined. The process for determining the SDC and other hazard variables is described in Chapter 3 of this thesis. The essential variables that describe the seismic hazard are shown in Table 6.1. After recording these values, the seismic forces required for design were calculated using the Equivalent Static Analysis (ESA) uniform load method described in the AASHTO Guide Specifications (AASHTO, 2011).

Table 6.1: Seismic Hazard Values

Bridge	A_S	S_{DS}	S_{D1}	SDC
Walker County	0.139g	0.293g	0.155g	B
Limestone County	0.132g	0.316g	0.177g	B
Montgomery County	0.067g	0.154g	0.104g	A

The first step in the ESA method is to determine the fundamental period of the bridge by running a Modal analysis on the bridge models. A Modal analysis will give the period for both the longitudinal and the transverse direction. As a note, Wu and Marshall (2018) conducted a parametric study of prestressed concrete girder bridges to determine a simplified method of estimating the period of a bridge. However, because steel bridges are much more variable in their parameters, this parametric study was not extended to include them. Thus, a Modal analysis using a computer model, or calculations in accordance with AASHTO Guide Specifications (2011), need to be completed for steel bridges. After determining the period, the design spectral acceleration (S_a) can be calculated from AASHTO Guide Specifications (2011) section 3.4.1. Next, the weight of the bridge can be determined by calculation. These values, along with the length of the bridge, were used in Equation 6.1 below to calculate the uniformly distributed load that is applied to the bridge. A distributed load is calculated both for the longitudinal direction and the transverse direction. This load represents the equivalent static forces that a seismic event would create on the bridge through dynamic inertial forces. The fundamental period, S_a, and the uniform load for each of the three bridges is shown in Table 6.2 below.

$$P_e = \frac{S_a * W}{L} \qquad \text{Equation 6.1}$$

Where P_e = Equivalent static uniform load
S_a = Design spectral acceleration

W = Weight of bridge
L = Length of bridge

Table 6.2: Equivalent Static Loads

Bridge	Longitudinal Period (sec)	Transverse Period (sec)	Longitudinal S_a (g)	Transverse S_a (g)	Longitudinal Uniform Load (k/ft.)	Transverse Uniform Load (k/ft.)
Walker County	1.33	0.626	0.117	0.248	1.58	3.35
Limestone County	0.724	0.682	0.244	0.259	2.49	2.64
Montgomery County	1.30	0.672	0.080	0.154	0.844	1.62

In lieu of calculating a period of vibration, the maximum spectral acceleration for determining the seismic forces, S_{DS}, can be used in the calculation of P_e, instead of the S_a value which is based on the period. With this method, the same uniform load will be applied in both directions. This allows the designer to transition directly from determining the seismic hazard to determining the equivalent static forces. The percent increases in load from the simplified S_{DS} selection as opposed to calculation of the period of vibration are shown in Table 6.3. It can be seen that the load does not increase at all for the transverse load of the Montgomery County bridge, but it increases by 158% for the longitudinal load of the Walker County bridge. All the other cases show an increase between these two values that vary from around 20% up to 92%. It should be noted that the increases are more significant for the bridges in the higher seismic zones.

Table 6.3: Simplified Uniform Loads

	Walker County	Limestone County	Montgomery County
Uniform Load from S_{DS} (kip/ft)	3.97	3.21	1.62
Longitudinal Uniform Load (k/ft.)	1.58	2.49	0.844
Longitudinal Percent Increase (%)	158	29.3	91.7
Transverse Uniform Load (k/ft.)	3.35	2.64	1.62
Transverse Percent Increase (%)	21.4	21.8	0

6.4.2 Analytical Bridge Models

It is important to get a general understanding of how the three-dimensional model was created in order to be more familiar with the overall analysis. The three bridges were modeled in CSiBridge 15 from the information given by the construction drawings, which allowed the overall geometry of the bridge to be specified. Details were input to define the overall layout, deck, girders, diaphragms, bearing connections, abutments, bents and bent caps, spans, and foundations.

The deck was modeled as an "area object model" which uses two-dimensional (shell) elements to represent the stiffness and strength of the deck. Frame elements were used to represent the girders' cross-sectional properties and material properties and were modeled in the same plane as the area elements of the deck. The diaphragms also used frame elements to represent the actual truss members and the chords and diagonals tied into nodes at the top and bottom of the girders. Because the girders were modeled within the plane of the deck, rigid link elements were used to represent the depth of the girders and were connected to the top and bottom nodes into which the diaphragms were framed.

Next, the bearing connections used link elements to represent the stiffness of the connection and were specified to link the bottom of the girders to the top of the bent cap. More details on this connection are provided in section 6.4.3. The substructure used frame elements for both the bent cap and the columns, and a moment connection was provided between the two. For all frame elements in the model, four-foot sections of the members were used to provide more precise results. Lastly, the foundation elements were represented as fixed connections at the bottom of the bents and abutments.

After creating a model of the structure, the equivalent seismic loads were applied to the deck. For the Walker County and Limestone County bridges, the longitudinal uniform load was placed at the center of the deck and loaded the entire bridge length. The transverse uniform load was placed on the edge of the deck perpendicular to the longitudinal axis and loaded the entire bridge length. However, because the Montgomery County bridge was curved, a different method of applying loads was used. Area loads were used instead of uniform loads, and these loads were applied to every area element within the deck. The loads were defined in the local axis directions of the area elements to ensure that the longitudinal loads remained parallel to the longitudinal axis and the transverse loads remained perpendicular to the longitudinal axis. The value of the area loads was calculated by dividing the uniform load values by the width of the deck. Figure 6.3 presents an example of the models with a cross section of the Walker County bridge at one of the bents. All of the structural elements discussed here can be seen in Figure 6.3. One note about Figure 6.3 is that the girders frame in and out of the page which makes the girders and other nodal points within the deck look similar. However, the

girders are only located above the rigid link elements. Figure 6.4 shows how the transverse seismic uniform loads were applied to the bridge deck.

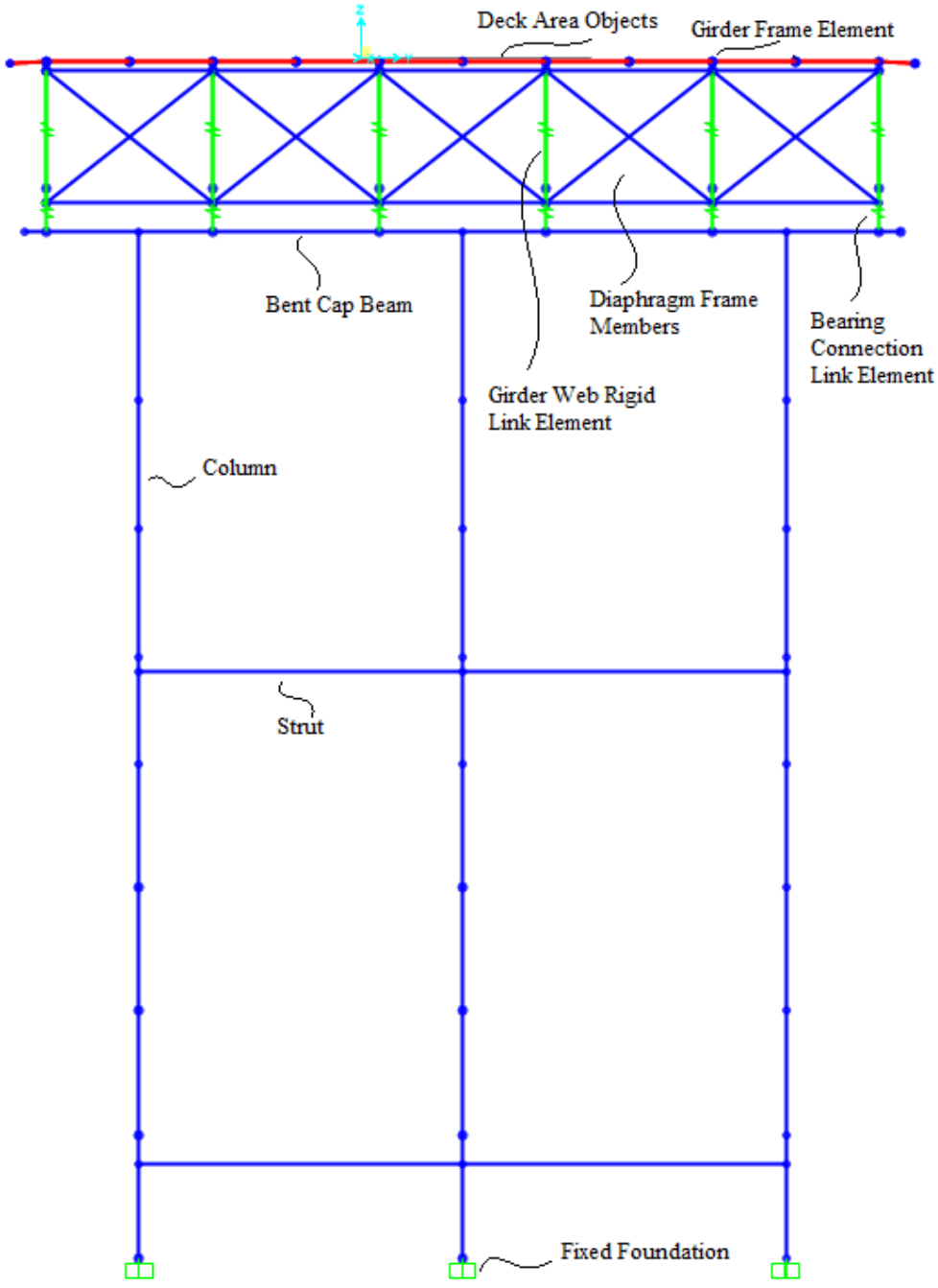

Figure 6.3: Walker County Bridge Cross Section

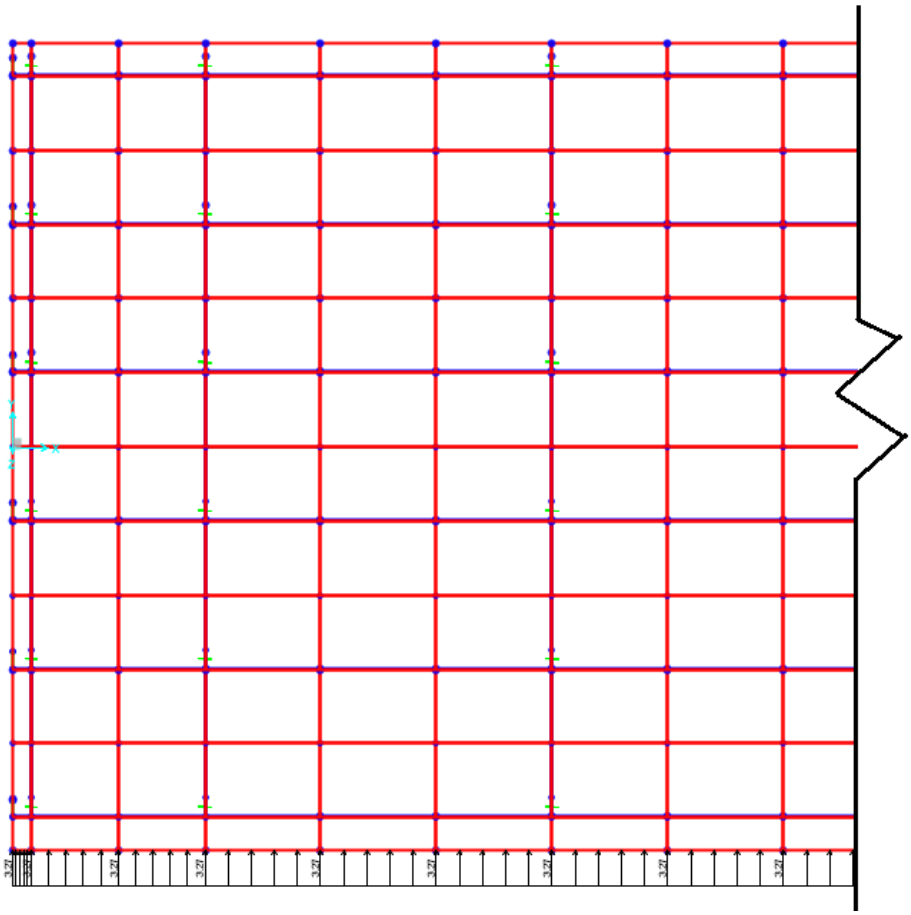

Figure 6.4: Transverse Seismic Loads

6.4.3 Elastomeric Bearing Models

To model the elastomeric bearing connection, it was important to be as accurate as possible in representing the stiffness of the connections. In order to calculate the stiffness of the connection in each direction, Equations 6.2 and 6.3 were used. Equation 6.2 represents the stiffness of the bearing pad alone, while Equation 6.3 represents the stiffness of the anchor bolts alone. The only component providing resistance in the longitudinal direction was the bearing pad, therefore only Equation 6.2 was used to calculate the longitudinal stiffness. The anchor bolts provide resistance in the transverse direction along with the bearing pad, therefore the stiffness for the transverse direction was the sum of both equations. The stiffness of the anchor bolts was calculated from the

stiffness of combined shear and flexural cantilever bending. The anchor bolts extend past the bent cap and span a gap between the bent cap and the sole plate. Therefore, it was determined that the anchor bolts would behave as a cantilever element. A value of 135 psi was used for the shear modulus (G) of the bearing pads based on a Caltrans (1994) design memo. All other values in the equations were recorded from the design drawings provided by ALDOT. The calculated stiffness for each bearing pad is provided in Table 6.4. Note that the Limestone County bridge has the same stiffness for the longitudinal direction as the transverse direction. This is because the connections for this bridge had no anchor bolts. This was an old connection from 1984 that ALDOT used, and they have since moved to the connection shown in Figure 6.1 that includes anchor bolts. To model the stiffness of all the connections, a link element was defined with partial fixity in the longitudinal and transverse directions. The value for the partial fixity was the stiffness calculated using Equations 6.2 and 6.3. The connection stiffness for all the bridge models are shown in Table 6.4.

$$k_{bearing} = \frac{G*A}{t} \qquad \text{Equation 6.2}$$

Where $k_{bearing}$ = Stiffness of bearing pad
G = Shear modulus of elasticity of bearing pad
A = Plan area of bearing pad
T = Thickness of bearing pad

$$k_{bolt} = \frac{3*E*I}{L^3} * N_b \qquad \text{Equation 6.3}$$

Where k_{bolt} = Stiffness of anchor bolt
E = Modulus of elasticity of anchor bolt
I = Moment of inertia of anchor bolt
L = Length of anchor bolt
N_b = Number of anchor bolts

Table 6.4: Stiffness of Elastomeric Bearings

Bridge	Connection Location	Longitudinal Stiffness (k/in.)	Transverse Stiffness (k/in.)
Walker County	Abutment 1	14.4	128
	Bent 2	24.5	401
	Bent 3	63.4	1880
	Bent 4	24.5	401
	Bent 5	14.4	128
	Abutment 6	14.4	128
Limestone County	Abutment 1	19.9	19.9
	Bent 2	18.5	18.5
	Bent 3	18.5	18.5
	Abutment 4	19.9	19.9
Montgomery County	Abutment 1	22.6	834
	Bents 2-6	13.2	236
	Bent 7	17.6	246
	Bents 8-9	40.5	852
	Abutment 10	22.6	834

6.4.4 Superstructure-to-Substructure Connection Design

After determining the equivalent uniform load, it was applied to the bridge model, and the structural analysis was run for both the longitudinal and transverse loads. CSiBridge 15 was used to determine the shear force induced by the uniform loads in the link elements that represented the elastomeric bearing connection. The shear force created by the dead load was also recorded and factored loads were calculated based on AASHTO LRFD Specifications Table 4.3.1-1 and 4.3.1-2 (LRFD, 2014). These values were calculated for each of the bents along each bridge, and the worst-case connection at each bent was chosen for design. The factored loads for both the longitudinal and transverse directions for every bent are shown in Table 6.5.

Table 6.5: Factored Connection Loads

Bridge	Connection Location	Factored Longitudinal Shear Force (k)	Factored Transverse Shear Force (k)
Walker County	Abutment 1	41.6	-41.9
	Bent 2	50.0	-117
	Bent 3	50.8	-180
	Bent 4	13.3	-85.1
	Bent 5	24.2	-74.8
Limestone County	Abutment 1	30.1	-25.3
	Bent 2	17.4	-24.8
	Bent 3	18.9	-24.8
	Abutment 4	30.1	-25.3
Montgomery County	Bent 7	12.7	-42.1
	Bent 8	31.2	-76.2
	Bent 9	30.9	-60.8
	Abutment 10	49.2	-28.6

Once the factored loads were determined, the strength of the welds connecting the girder to the sole plate was calculated. Different values such as the length of the weld, the weld size, the weld yield strength, and sole plate thickness were obtained from the design drawings. Three limit states were checked to determine the overall strength of the welded connection: base metal yielding on the gross section and rupture on the net section (LRFD, 2014, p. 6-235), base metal shear failure (LRFD, 2014, p. 6-235), and weld metal shear rupture (LRFD, 2014, p. 6-232). The equations used to calculate these are shown as Equations 6.4-6.6, respectively. The limit state that gave the lowest resistance was recorded as the capacity of the welded connection. This capacity was then compared to the factored shear demand from Table 6.5. These values are shown below in Table 6.6.

$$\phi R_n = \phi_y F_y A_g \leq \phi_u F_u R_p A_n U \qquad \text{Equation 6.4}$$

Where ϕR_n = Nominal resistance of base metal in tension
ϕ_y = Resistance factor for yielding of tension members
F_y = Base metal yield stress

A_g = Gross connection area
ϕ_u = Resistance factor for fracture of tension members
F_u = Base metal minimum tensile strength
R_p = Reduction factor for holes
A_n = Net connection area
U = Shear lag factor

$$\phi R_n = 0.58\phi_v F_y A_g \qquad \text{Equation 6.5}$$

Where ϕR_n = Nominal resistance of base metal in shear
ϕ_v = Resistance factor for base metal shear

$$\phi R_n = 0.6\phi_{e2} F_{exx} A \qquad \text{Equation 6.6}$$

Where ϕR_n = Nominal resistance of weld shear rupture
ϕ_{e2} = Resistance factor for weld metal shear rupture
F_{exx} = Yield stress of weld
A = Connection area

Table 6.6: Connection Weld Capacities

Bridge	Connection Location	Weld Capacity (k)	Adequate Capacity?
Walker County	Abutment 1	143	Yes
	Bent 2	261	Yes
	Bent 3	261	Yes
	Bent 4	261	Yes
	Bent 5	143	Yes
Limestone County	Abutment 1	91.6	Yes
	Bent 2	91.6	Yes
	Bent 3	91.6	Yes
	Abutment 4	91.6	Yes
Montgomery County	Bent 7	238	Yes
	Bent 8	356	Yes
	Bent 9	356	Yes
	Abutment 10	238	Yes

The other part of the superstructure-to-substructure connection that needed to have its capacity calculated was the anchor bolts. Before calculating the capacity though, it was determined that the anchor bolts would be subjected to flexural demand as well as

shear demand. This is because the anchor bolts extend from the bent cap through the bolt holes in the sole plate. The nut that is placed on the anchor bolts is not tightened to the sole plate completely, so there is a 1/8 in. gap between the nut and the sole plate. This will cause the bolt to bend as a cantilever element and be subjected to significant flexural demand. Additionally, the AASHTO Guide Specifications explicitly state, "The anchor bolts shall be designed for the combined effect of bending and shear for seismic loads" (AASHTO, 2011).

To determine the flexural demand of the anchor bolts, the behavior of the bending needed to be investigated. While the stiffness and the initial behavior was based on a cantilever element, it was determined that eventually the top of the anchor bolt would come into contact with the sole plate and cause moment to be developed there. Therefore, the first step in determining the flexural demand was to calculate the required shear force that would cause the anchor bolt to deflect 0.25 in. at the top. 0.25 in. represents the difference between the width of the slotted holes and the diameter of the anchor bolt. This value could vary, but the examples given by ALDOT were consistent with a 0.25 in. gap. After deflecting 0.25 in., the anchor bolt would contact the sole plate.

After determining the amount of shear force that would cause the anchor bolt to deflect 0.25 in., this force was compared to the total shear force at the bearing connection. If the total shear force was less than the calculated force, then the anchor bolt would not come into contact with the sole plate and would behave as a cantilever element completely. However, if the total shear force was more than the calculated force, then the calculated force would cause moment at the base of the anchor bolt equal to the calculated force multiplied by the length of the anchor bolt as defined above. The

remaining shear force at the bearing connection would then continue to bend the anchor bolt similar to having a fixed-fixed connection. Therefore, the rest of the moment developed at the base of the anchor bolt could be calculated by multiplying the remaining force by half the length of the anchor bolt. It is important to note that the length of the anchor bolts ranged anywhere from around three inches to over seven inches which caused significant bending moments to be developed in the anchor bolt. These moments can be seen in Table 6.7. As previously stated, the Limestone County bridge did not have anchor bolts as part of the connection so there were no bending moments developed.

Table 6.7: Anchor Bolt Bending Moments

Bridge	Connection Location	Anchor Bolt Bending Moment (kip*in)
Walker County	Abutment 1	-304
	Bent 2	-715
	Bent 3	-651
	Bent 4	-521
	Bent 5	-542
Limestone County	Abutment 1	N/A
	Bent 2	N/A
	Bent 3	N/A
	Abutment 4	N/A
Montgomery County	Bent 7	-303
	Bent 8	-362
	Bent 9	-289
	Abutment 10	-136

After determining the flexural demand, the flexural and shear capacities of the anchor bolts were calculated. An interaction equation for the combination of flexure and shear loading was sought, but after considerable research, a sufficient equation was not able to be found. Thus, the flexural and shear capacities were calculated separately. The flexural capacity was calculated using Equation 6.7, which was based on flexural yielding

alone because lateral torsional buckling does not apply to solid round bars (LRFD, 2014, p. 6-212). The elastic section modulus and the plastic section modulus had to be calculated for the anchor bolts, and Equations 6.8 and 6.9 show the method for these calculations. Finally, the shear strength was calculated with Equation 6.10, and all capacities were compared to the corresponding flexural and shear demand from Tables 6.4 and 6.6. The capacities are shown in Table 6.8 below.

$$\phi M_n = \phi_f F_y Z \leq \phi 1.6 F_y S \qquad \text{Equation 6.7}$$

Where ϕM_n = Nominal moment resistance
ϕ_f = Resistance factor for flexural bending
F_y = Yield stress of anchor bolt
Z = Plastic section modulus
S = Elastic section modulus

$$Z = \frac{D^3}{6} \qquad \text{Equation 6.8}$$

$$S = \frac{\pi D^3}{32} \qquad \text{Equation 6.9}$$

Where D = Diameter of anchor bolt

$$\phi R_n = 0.48 A_b F_{ub} N_s \qquad \text{Equation 6.10}$$

Where A_b = Area of anchor bolt
F_{ub} = Minimum tensile strength of anchor bolt
N_s = Number of shear planes per anchor bolt

Table 6.8: Flexural and Shear Capacities of Anchor Bolts

Bridge	Connection Location	Flexural Capacity (kip*in)	Adequate Capacity?	Shear Capacity (kip)	Adequate Capacity?
Walker County	Abutment 1	63.6	No	76.3	Yes
	Bent 2	127	No	153	Yes
	Bent 3	127	No	153	No
	Bent 4	127	No	153	Yes
	Bent 5	127	No	76.3	Yes
Limestone County	Abutment 1	N/A	N/A	N/A	N/A
	Bent 2	N/A	N/A	N/A	N/A
	Bent 3	N/A	N/A	N/A	N/A
	Abutment 4	N/A	N/A	N/A	N/A
Montgomery County	Bent 7	127	No	204	Yes
	Bent 8	127	No	204	Yes
	Bent 9	127	No	204	Yes
	Abutment 10	63.6	No	102	Yes

6.5 Discussion

After investigating the welded connection, it was determined that all welds had adequate capacity to resist the shear force being transferred. The connection with the highest shear demand was Bent 3 in the Walker County bridge, but the weld's capacity exceeded the demand by over 80 kips. The anchor bolts also performed well in shear resistance with all but one bolt containing enough capacity. Bent 3 for the Walker County bridge had its capacity exceeded by 29 kips, resulting in the anchor bolts failing. However, this is not necessarily a problem with the design of the connection itself, rather, it means that extra care needs to be given to the selection of bolt sizes. Increasing the anchor bolts' diameter by only a quarter of an inch would provide enough capacity to resist the shear demand. It should be noted, however, that the elastomeric bearing pad most likely will absorb some of the shear force as well instead of the full force being applied to the anchor bolts. Still, AASHTO Guide Specifications (2011) state that

elements resisting force through friction should not be considered to provide beneficial resistance in design. Thus, the anchor bolts were considered to resist the full shear force in this thesis.

While the connection performs well in resisting shear, the anchor bolts do not have nearly enough flexural capacity. The flexural demand exceeded the capacity from anywhere between 73 kip-in. to 588 kip-in. The simplest solution to this would be to increase the bolt's diameter. However, to achieve enough strength to resist the demand of the Walker County bridge, the anchor bolts would need to be 3.25 inches at the worst case bent. It may be unrealistic to provide anchor bolts of this size so another solution was investigated.

6.6 Recommendation

As previously stated, clear guidance for the design of combined shear and flexural loads in anchor bolts was not found; therefore, an alternate design was investigated to resist the transverse movement of the superstructure. Shear blocks, or girder stops, were chosen for this design and, although anchor bolts are still required for the design of elastomeric bearing connections (LRFD, 2014), they will act as redundant resistance to the transverse forces if the anchor bolts fail. Shear blocks are short blocks of reinforced concrete that are cast monolithically to the top of the bent cap between two girders. The Federal Highway Administration (FHWA, 2011) provided the following guidance for girder stops:

> The girder stop will act as secondary restraint members. The girder stops should not participate under service or the design seismic load conditions. A girder stop should exist between each girder line. A gap should be provided between the load

> plate of the bearing assembly and the girder stop equal to design displacement in the transverse direction…It is common to design each girder stop for a force equal to the total bearing shear demands at a pier. This is because the girder stops don't always engage simultaneously. Under this condition, the girder stop contacted first could be overloaded and fail before the other girder stops are engaged. This could lead to an "unbuttoning" effect of the girder stops.

The "unbuttoning" effect described here is the consecutive failure of each shear block caused by the superstructure contacting only one block at a time. This conservatively assumes that the entire base shear of the bent will be resisted by one block. Based on this guidance, a design example was created for abutment 10 of the Montgomery County bridge. This section will detail the procedure for design of shear blocks.

6.6.1 Shear Block Design Procedure

To ensure that the design and construction of the shear blocks is as simplified as possible, it is recommended that only one shear block be used between two of the girders near the center of the bent. The dimensions of the shear block can usually be determined outright—or at least a close estimation can be made. The height (h) of the shear block can be determined by adding the concrete cover length to the distance between the top of the sole plate and the top of the bent cap. The length (l_v) of the shear block can be assumed to be the width of the bent cap. Finally, the width (w) of the sole plate can be estimated by the clear distance of adjacent girder sole plates minus a gap determined by the designer. The recommendation from the FHWA (2011) was to make the gap as large as the design displacement in the transverse direction. Figure 6.5 shows what the different dimensions

of the shear block represent. The length of the shear block is not shown in Figure 6.5 because it is in and out of the page.

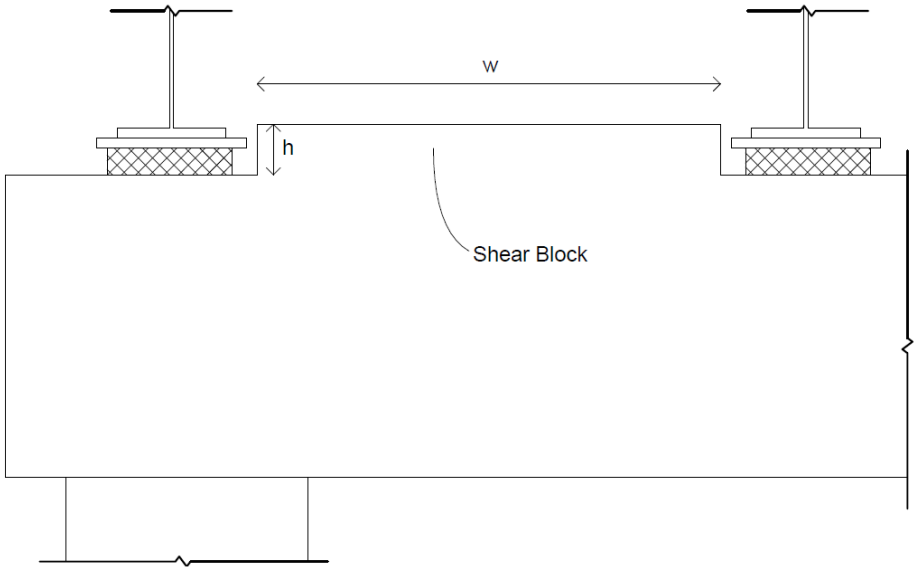

Figure 6.5: Shear Block

In order to ensure the shear block has adequate strength and is able to transfer the shear into the bent cap, shear friction reinforcement was provided at the interface between the shear block and the bent cap. LRFD Specifications (2014) state that shear friction reinforcement must be provided across a given plane at:

- An existing or potential crack
- An interface between dissimilar materials
- An interface between two concretes cast at different times
- The interface between different elements of the cross section

The shear resistance for the plane between the shear block and bent cap can be determined using Equation 6.11. Upon investigation of this equation, the shear resistance provided by the concrete is very large because the plan dimensions of the shear block are very large. According to the calculation, the concrete was able to resist the base shear at

abutment 10 of the Montgomery County bridge without any shear friction reinforcement. However, a minimum amount of reinforcement is required based on Equation 6.12. After determining the minimum amount of reinforcement required, the total shear resistance was calculated again using Equation 6.11. This resistance was then compared to two design checks shown in Equations 6.13 and 6.14. One interesting note is that if the shear strength was calculated only using the resistance of the minimum required shear friction reinforcement in Equation 6.11, the resistance of the reinforcement alone would be adequate to resist the base shear at abutment 10.

$$\phi_{shear} V_n = \phi_{shear} c A_{cv} + \mu A_{vf} f_y \qquad \text{Equation 6.11}$$

Where ϕ_{shear} = Resistance factor for shear
V_n = Nominal shear resistance
c = Cohesion factor
c = 0.4 ksi for concrete cast monolithically
A_{cv} = Area of concrete considered to be engaged in interface shear transfer
μ = Friction factor
μ = 1.4 for concrete cast monolithically
A_{vf} = Area of shear friction reinforcement
f_y = Yield stress of shear friction reinforcement

$$A_{vf,min} \geq \frac{0.05 A_{cv}}{f_y} \qquad \text{Equation 6.12}$$

Variables previously defined.

$$V_n \leq K_1 f'_c A_{cv} \qquad \text{Equation 6.13}$$

Where K_1 = Fraction of concrete available to resist interface shear
K_1 = 0.25 for concrete cast monolithically
f'_c = Compressive strength of concrete

$$V_n \leq K_2 A_{cv} \qquad \text{Equation 6.14}$$

Where K_2 = Limiting interface shear resistance
K_2 = 1.5 ksi for concrete cast monolithically

The shear friction reinforcement was provided in two rows along the edges of the shear block (left and right sides in Figure 6.5). In order to aid in constructability and to

control cracking, two transverse reinforcement tie layers were provided within the shear block. The shear friction reinforcement was also specified to be hooked within the shear block to ensure adequate development. The details for the design of the shear block are provided in Table 6.9.

Table 6.9: Shear Block Design Details

Length (in.)	60
Width (in.)	78
Height (in.)	10
Shear Demand (kip)	281
Interface Shear Capacity (kip)	1980
Number of Shear Friction Bars	14 (7 each side)
Size of Shear Friction Bars	#5
Shear Reinforcement Spacing (in.)	9

It can be seen from this table that the shear block's capacity is far greater than the demand. This is because the shear block is designed with large dimensions but is only lightly reinforced. In order to save materials, the designer could design two smaller shear blocks that are more heavily reinforced that would be placed on the interior side of two adjacent girders. However, because ALDOT desires simplification, it is recommended that the design method with a single shear block as described above be followed.

6.7 Summary

The purpose of this task was to verify whether the current superstructure-to-substructure connection that ALDOT uses is adequate to resist seismic loads. The

strength and demand were calculated for both the welded part of the connection and the anchor bolt part of the connection. While the welded connection had adequate capacity, the anchor bolt connection was greatly under-designed for flexural resistance. Thus, a recommendation was made to provide shear blocks at the bents between girders. These shear blocks provide a secondary resistance to transverse movement of the superstructure if the anchor bolts fail during ground motions. An example design from abutment 10 of the Montgomery County bridge was provided to show the design process of the shear keys. Overall, if the guidance in this section is followed, the superstructure-to-substructure connection will provide adequate resistance for seismic events.

Chapter 7: End Diaphragm of Steel Girder Bridges

7.1 Introduction

Another critical element of steel girder bridges is the diaphragms, or cross frames, that are spaced throughout each span and at the supports. These are typically made up of a truss system that resists loads axially, but they can also be made of a beam element that will resist loads in flexural bending. The truss system type is the most common and will be studied in this report as ALDOT only provided examples of this type of diaphragm. The diaphragms span between the bridge girders with a top and bottom chord located near the top and bottom flanges of the girder and diagonal bracing between the chords.

The main purpose of diaphragms is to prevent twisting of the bridge girders which are heavily susceptible to lateral-torsional buckling (Helwig & Wang, 2003). The truss configuration of the diaphragms allows the elements in the truss to resist twisting of the bridge girders through axial loads in those elements. Depending on whether the diaphragm is located at the support (referred to here as “end diaphragms”) or between the supports (referred to here as “intermediate diaphragms”), the main cause of this movement has different sources. Intermediate diaphragms mainly resist movement caused by truck live loads as they move along the bridge (Helwig & Wang, 2003). Conversely, end diaphragms mainly resist movement caused by lateral loads on the bridge structure (Zahrai & Bruneau, 1998). Consequently, end diaphragms generally resist much larger loads than intermediate diaphragms, and they will be the focus of this study.

7.2 ALDOT's End Diaphragms

ALDOT does not have a standard system that they use for an end diaphragm because steel girder bridges vary widely in their parameters. However, the diaphragms from the three bridges studied have many similarities and are shown below in Figures 7.1-7.3. The Walker County diaphragm uses a single angle as the top chord and an X-brace as the configuration for the diagonals. It uses gusset plates to connect all truss members to the bearing stiffeners. The Limestone and Montgomery County diaphragms are similar—both using a channel section for the top chord and single angles for the bottom chord and diagonals. They both also use a chevron type configuration for the diagonals. The main difference between the Limestone and Montgomery diaphragms is that the Limestone County diaphragm connects all truss members directly to the bearing stiffeners whereas the Montgomery County diaphragm uses gusset plates to attach the diagonals and bottom chord to the transverse stiffeners and girder.

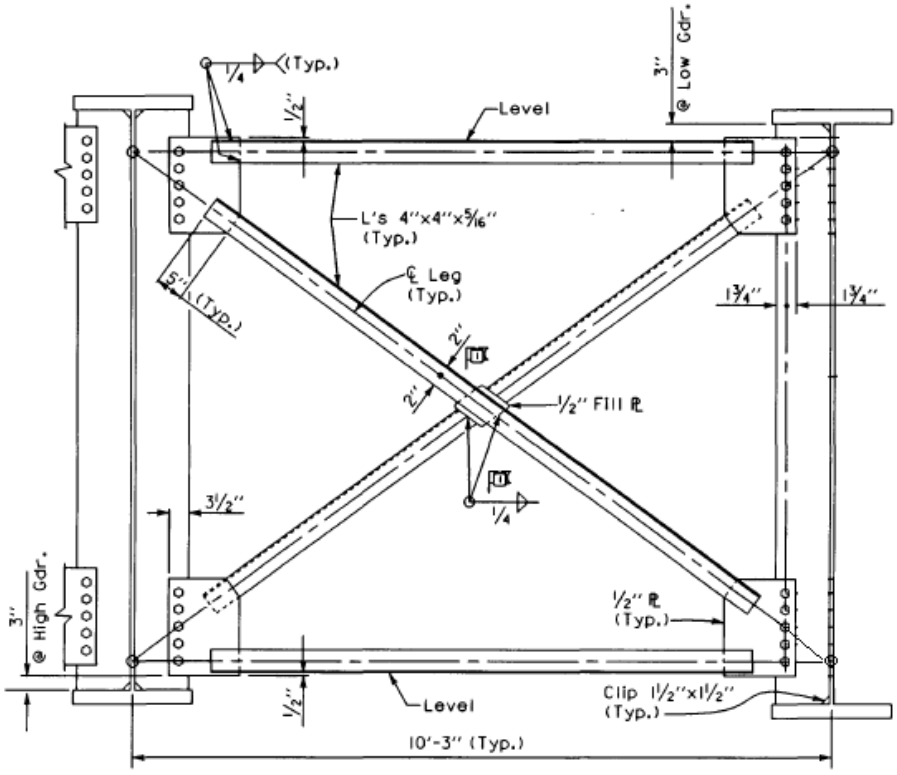

Figure 7.1: Walker County End Diaphragm (ALDOT, 2018)

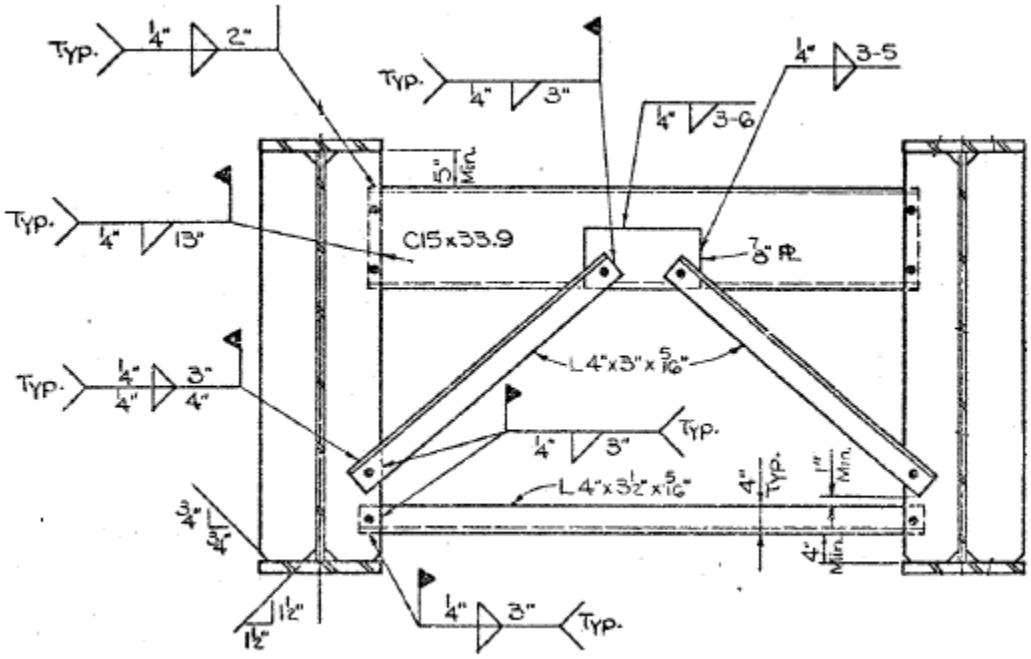

Figure 7.2: Limestone County End Diaphragm (ALDOT, 2018)

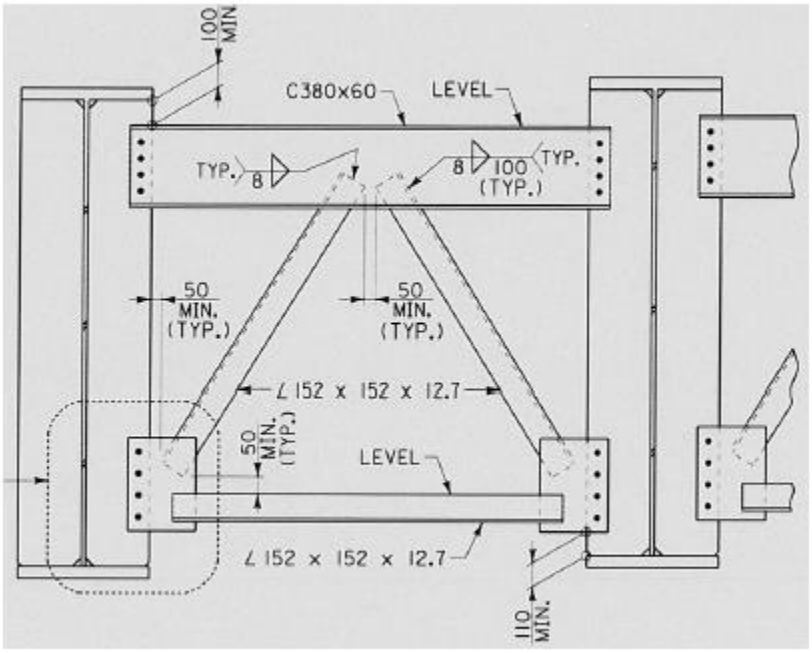

Figure 7.3: Montgomery County End Diaphragm (metric units) (ALDOT, 2018)

7.3 End Diaphragm Model

The analytical diaphragm model within CSiBridge 15 was created using the diaphragm tool in the software. This tool creates frame elements to represent the truss members and ties the chords and diagonals into nodes at the top and bottom of the girders. Because the girders were modeled within the plane of the deck, rigid link elements were used to represent the depth of the girders and connected the top and bottom nodes into which the diaphragms were framed. The size of the truss elements was recorded from Figures 7.1-7.3 and specified within the model. The same bridge models as described in Chapter 6 of this thesis were used along with the same seismic forces. Figure 7.4 presents an example of one set of diaphragms from the Walker County bridge that displays the internal axial forces of the truss members. This figure shows the diagonals that were over capacity as described in the next section.

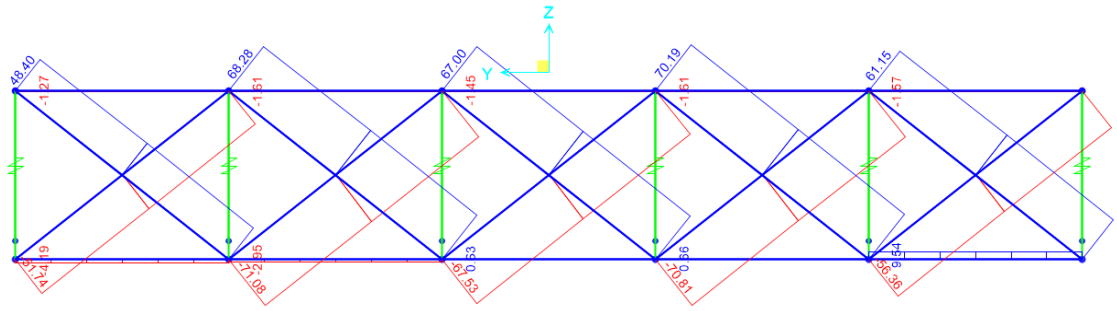

Figure 7.4: Walker County Diaphragm Axial Forces

7.4 End Diaphragm Design

After the analysis, the maximum compressive force and maximum tensile force was recorded for the top chord, the bottom chord, and the diagonals. These forces were used to design each member as a compression member and a tension member. The tension members were designed for yielding on the gross section, fracture on the net section, and block shear failure whereas compression members were designed for flexural buckling and/or flexural torsional buckling. The equations for yielding on the gross section and rupture on the net section are shown in Equation 6.4. The equation for block shear failure is shown in Equation 7.1. The overall tensile strength of the truss member was taken as the lowest value calculated from these equations.

$$\phi R_n = \phi_{bs} R_p (0.58 F_u A_{vn} + U_{bs} F_u A_{tn}) \leq \phi_{bs} R_p (0.58 F_y A_{vg} + U_{bs} F_u A_{tn}) \quad \text{Equation 7.1}$$

Where ϕ_{bs} = Resistance factor for block shear failure
R_p = Reduction factor for bolt holes
F_u = Minimum tensile strength
A_{vn} = Net area along the plane resisting shear stress
U_{bs} = Reduction factor for block shear rupture resistance
A_{tn} = Net area along the plane resisting tension stress
F_y = Minimum yield strength
A_{vg} = Gross area along the plane of resisting shear stress

The method of designing the members for compression was dependent on whether the member was a single angle or a channel section. For a channel section, the

equations for singly symmetric open-section members for flexural buckling and flexural torsional buckling apply (LRFD, 2014, p. 6-86). The first step in calculating the capacity of a channel section is to ensure that the cross section is not slender. The first slenderness limit is specified as 120 and is compared to the ratio between the unbraced length (L_b) and the radius of gyration of the y-axis. The second slenderness limit is shown in Equation 7.2 below. If this limit is not met, then the slender element reduction factor (Q) must be calculated; but if it is met, then Q is taken as 1.0 (LRFD, 2014, p. 6-92). After determining the slenderness of the section, the elastic critical buckling resistance (P_e) of the member can be calculated using Equation 7.3 below. This equation uses several variables that require their own calculation, so the equations for those variables follow Equation 7.3. Finally, the compressive capacity of the member can be calculated using Equation 7.8. This equation is only used when the ratio between the equivalent nominal yield resistance (P_0) to P_e is lower than 0.44; otherwise, Equation 7.9 is used.

$$\frac{b}{t} \leq k\sqrt{\frac{E}{F_y}} \qquad \text{Equation 7.2}$$

Where b = Distance specified in Table 6.9.4.2.1-1 of the LRFD Specifications (2014)
t = Thickness of flange, web, or leg
k = Constant specified in Table 6.9.4.2.1-1 of the LRFD Specifications (2014)

$$P_e = \left(\frac{P_{ey}+P_{ez}}{2H}\right)\left(1-\sqrt{1-\frac{4P_{ey}P_{ez}H}{\left(P_{ey}+P_{ez}\right)^2}}\right) \qquad \text{Equation 7.3}$$

Where P_e = Elastic critical buckling resistance

$$P_{ey} = \frac{\pi^2 E}{\left(\frac{K_y l_y}{r_y}\right)^2} A_g \qquad \text{Equation 7.4}$$

Where P_{ey} = Elastic critical buckling resistance of y-axis
$K_y l_y$ = Effective length factor of y-axis
r_y = Radius of gyration about the y-axis

$$P_{ez} = \left(\frac{\pi^2 E C_w}{(K_z l_z)^2} + GJ\right)\frac{1}{{r_0}^2} \quad \text{Equation 7.5}$$

Where P_{ez} = Elastic critical buckling resistance of y-axis
C_W = Warping torsional constant
$K_z l_z$ = Effective length for torsional buckling
G = Shear modulus of elasticity
J = St. Venant torsional constant

$${r_0}^2 = {y_0}^2 + \frac{I_x + I_y}{A_g} \quad \text{Equation 7.6}$$

Where r_0 = Polar radius of gyration about the shear center
y_0 = Distance along the y-axis between the shear center and centroid
I_x = Moment of inertia about the x-axis
I_y = Moment of inertia about the y-axis

$$H = 1 - \frac{{y_0}^2}{{r_0}^2} \quad \text{Equation 7.7}$$

Variables previously defined

$$\phi P_n = \phi_c 0.877 P_e \quad \text{Equation 7.8}$$

Where ϕP_n = Factored nominal compressive resistance
ϕ_c = Resistance factor for flexural buckling

$$\phi P_n = \phi_c \left(0.658^{\left(\frac{P_0}{P_e}\right)}\right) P_0 \quad \text{Equation 7.9}$$

Variables previously defined

For the single angle sections, the LRFD Specifications (2014) provide an approximate calculation in which there is no requirement to check flexural torsional buckling; only flexural buckling applies. This approximation can be used when the single angles meet certain criteria (LRFD, 2014, p. 6-96):

- End connections are to a single leg of the angle and are welded or use a minimum of two bolts;
- The angle is loaded at the ends in compression through the same leg;

- The angle is not subjected to any intermediate transverse loads;
- If used as web members in trusses, all adjacent web members are attached to the same side of the gusset plate or chord.

The commentary of section 6.9.4.4 in the LRFD Specifications mentions that this approximation generally applies to all single angles in diaphragms in a bridge system (LRFD, 2014, p. 6-96). When observing the above diaphragm drawings, it can be seen that they meet all of the requirements to use the approximate method.

The first steps in designing a single angle for compression follows the same process as the channel sections above—the slenderness limits and slenderness reduction factor must be checked and determined. After these are determined, the P_e can be calculated using Equation 7.10, then the factored nominal compressive resistance can be calculated with Equations 7.8 and 7.9. Essentially, the difference in this method is that only flexural buckling is being calculated using an alternative effective slenderness ratio. After calculating the resistance for the channels and single angles, the design of the diaphragm was complete. All compressive and tensile demand forces and capacities for each type of truss member for each bridge are shown in Table 7.1.

$$P_e = \frac{\pi^2 E}{\left(\frac{Kl}{r}\right)_{eff}} A_g \qquad \text{Equation 7.10}$$

Where $\left(\frac{Kl}{r}\right)_{eff} = \left(32 + 1.25\frac{K_x l_x}{r_x}\right)$ if $\frac{K_x l_x}{r_x} > 80$ Equation 7.11

or $\left(\frac{Kl}{r}\right)_{eff} = \left(72 + .75\frac{K_x l_x}{r_x}\right)$ if $\frac{K_x l_x}{r_x} \leq 80$ Equation 7.12

$K_x l_x$ = Effective length factor of x-axis
r_x = Radius of gyration about the x-axis

Table 7.1: Diaphragm Members Demand and Capacity

Bridge	Truss Member	Max Compressive Force (kip)	Compressive Capacity (kip)	Max Tensile Force (kip)	Tensile Capacity (kip)	Adequate Capacity?
Walker County	Top Chord	2.20	81.2	1.00	66.8	Yes
	Bottom Chord	12.6	81.2	14.5	66.8	Yes
	Diagonal	71.1	81.2	70.2	66.8	No
Limestone County	Top Chord	16.7	316	15.7	285	Yes
	Bottom Chord	5.00	76.3	6.10	62.6	Yes
	Diagonal	19.8	76.3	20.0	62.6	Yes
Montgomery County	Top Chord	9.50	326	1.40	150	Yes
	Bottom Chord	9.20	196	10.1	161	Yes
	Diagonal	45.5	196	48.1	161	Yes

7.5 Summary

The purpose of this task was to ensure that the end diaphragms used in ALDOT's bridges were adequate to resist seismic loads. Three different diaphragms were considered and modeled to analyze the force demand in the truss members. After calculating the capacities of each member, it was determined that all but one of the members that make up the truss diaphragms had adequate capacity. One of the diagonal members in the Walker County bridge failed in tension by 3.4 kips. This does not mean that the overall design of the diaphragms is inadequate. It means that a larger member was needed for the diagonals of that truss so that it would remain elastic. Comparison of the rest of the members shows that most of them had a much larger capacity than was needed. Besides the diagonals of the Walker County bridge, the largest demand to capacity ratio was 0.32. Although the strength of the diaphragms was in general much higher than needed, the stiffness of the diaphragms could have been the controlling factor in their design. If torsional deformations were too large, a stiffer diaphragm could have

been needed to prevent the girders from twisting. Whether this is true or not is difficult to determine in a post-design analysis, so it was not investigated further.

Chapter 8: Summary, Conclusions, and Recommendations

8.1 Summary

The objective of this thesis was to provide new and investigate current design details and procedures for the seismic design of standard bridges in the state of Alabama. Because of the low to moderate seismic hazard in the state, it was desired to reduce the time required to meet the seismic design requirements of the AASHTO Guide Specifications and LRFD Specifications. Five main topics were discussed in this thesis with the first topic being the development of seismic hazard maps for the state of Alabama by county. These maps will enable designers to quickly determine the level of seismic detailing needed for a particular bridge. The second topic discussed was the development of standard drawings for the plastic hinge zone in reinforced concrete columns. Standard drawings will aid in the efficiency of the designer's work by quickly presenting the requirements of the reinforcement inside the plastic hinge zone. The third topic covered was determining the calculations required for support length. After investigating whether the bridges studied were in danger of becoming unseated, it was determined that using the AASHTO Guide Specifications for calculating seat length is adequate. The fourth topic studied was the validation of ALDOT's current superstructure-to-substructure connection. Analytical models were created, and a static analysis was conducted to determine the demand on the connection. The load path of the connection was evaluated to determine if it was complete in the transfer of forces between the superstructure and substructure. Finally, validation of the end diaphragms of steel girder

bridges was made by determining the forces within each truss element and designing each element as a compression and tension member.

8.2 Conclusions

Based on the analysis performed in this thesis, the following conclusions can be made about the simplification and standardization of seismic design procedures:

- Alabama's seismic hazard is noticeably higher nearer the northern part of the state due to the New Madrid and Eastern Tennessee Seismic Zones.
- A minimum aspect ratio (ratio of length to maximum width) of 4.0 needs to be used in SDC B or greater for the reinforced concrete columns of bridges to ensure adequate space is provided for splicing reinforcement outside the plastic hinge zone.
- The equation in the AASHTO Guide Specification for support length provides adequate support length for the hazard that is present in Alabama. The support length will allow the superstructure to "ride out" the ground motions and prevent the girders from becoming unseated which was a risk because the superstructure-to-substructure connection does not have a complete load path in the longitudinal direction.
- The anchor bolts in the superstructure-to-substructure do not provide adequate strength to resist transverse seismic loads.
- Most of the members in the end diaphragms of the three bridges studied provide enough capacity; however, one member did fail in tension. End diaphragms provide resistance to lateral loads and therefore need to be designed for seismic loads. Because most of the members in the truss are over-designed, including

seismic loads in the analysis should not significantly change the sizes of most of the truss members.

8.3 Recommendations

Based on the conclusions above and the analysis done in this thesis, the following recommendations can be made to improve the seismic design process for ALDOT:

- A minimum aspect ratio (ratio of length to maximum width) of 4.0 is recommended in SDC B or greater for reinforced concrete columns to ensure enough space for splicing of reinforcement.
- ALDOT should use the equation for support length from the AASHTO Guide Specifications to calculate the support length required for a bridge span.
- A shear block should be provided at abutments and bents between two interior girders. This will provide resistance to transverse movement of the superstructure in case the anchor bolts fail.
- Because shear blocks are being recommended to resist transverse motion, the anchor bolts in the superstructure-to-substructure can be limited to the design for other loads besides seismic.
- End diaphragms need to be designed for seismic loads, and in order to achieve material and financial savings, a more optimized design of the end diaphragms is suggested.

8.4 Further Research

Certain parts of this thesis could benefit greatly from additional research. First, the determination that the equation for support length in the AASHTO Guide Specifications is adequate was based on research that only studied prestressed concrete

girder bridges with simple spans. To extend this recommendation to steel bridges, analyses similar to Law (2013) and Panzer (2013) should be conducted for steel girder bridges. Second, the assumption was made that the bearing connections become ineffective when half the bearing pad extends past the edge of the bent cap. Research should be conducted to find the point that the bearing pad actually becomes ineffective. Third, the design of anchor bolts under combined shear and flexural loading is largely unstudied. Further research should be funded to understand how these anchor bolts behave under lateral loads. Finally, the axial forces within the end diaphragm trusses reported in this thesis were only determined based off factored dead and seismic load. Live load created by trucks and vehicles could have significant impact on the demand of these members. While AASHTO LRFD Specifications do not explicitly require the combined effects of live load and seismic loads, the commentary suggests using 50% of the live load if the designer deems it necessary. Thus, a study that included this live load would be beneficial to determine if any more of the members are over capacity.

References

AASHTO. (2011). *Guide Specifications for LRFD Seismic Bridge Design* (2nd ed.). Washington DC: American Association of State Highway and Transportation Officials.

AASHTO. (2014). *LRFD Bridge Design Specifications* (4th ed.). Washington DC: American Association of State Highway and Transportation Officials.

Alabama DOT. (2012, November 30). *ALDOT Standard Details.* Alabama Department of Transportation.

ATC/MCEER Joint Venture. (2003). *Recommended LRFD Guidelines for the Seismic Design of Highway Briges.* Federal Highway Administration.

Autodesk. (2018). *Autodesk Revit 2018 [computer software]*.

Caltrans. (1994, June). Bridge Bearings. *Memo to designers 7-1*, pp. 1-12.

Chen, W.-F., & Duan, L. (2000). *Bridge Engineering Seismic Design.* Boca Raton: CRC Press.

Computer and Structures Inc. (2012). *CSI Bridge 15.* Berkely, CA: Computer and Structures, Inc.

Corporation, P. T. (2007). *Mathcad 14.* Needham, MA: Parametric Technology Corporation.

FHWA. (2011). *LRFD Seismic Analysis and Design of Bridges Design Examples.* New York.

GOOGLE. (2018). *Google Maps.* [Graph illustration of United States map]. Retrieved from https://www.google.com/maps.

Helwig, T. A., & Wang, L. (2003). *Cross-Frame and Diaphragm Behavior for Steel Bridges with Skewed Supports.* Houston, Texas: University of Houston.

Konstantinidis, D., Kelly, J. M., & Makris, N. (2008). Experimental Investigation on the Seismic Response of Bridge Bearings. Berkley, California.

Law, J. D. (2013). *Update of Bridge Design Standards in Alabama for AASHTO LRFD Seismic Design Requirements.* Auburn, AL: Auburn University.

Mander, J. B. (1983). *Seismic Design of Bridge Piers.* Christchurch, New Zealand: University of Canterbury.

Mander, J. B., Kim, D.-K., Chen, S. S., & Premus, G. J. (1996). *Response of Steel Bridge Bearings to Reversed Cyclic Loading.* Buffaly, New York: National Center for Earthquake Engineering Research.

Mapchart. (2018). *State of Alabama Map.* [Graph illustration of State of Alabama map]. Retrieved from https://mapchart.net/usa-counties.html.

Panzer, J. (2013). *Evaluation of Critical and Essential Concrete Highway Bridges in a Moderate Seismic Hazard.* Auburn, AL: Auburn University.

United States Geological Survey. (2018). *U.S. Seismic Design Maps.* [Graph illustration of Seismic Design Maps July, 2018]. Retrieved from https://earthquake.usgs.gov/designmaps/us/application.php?

Wu, H., Marshall, J., & Broderick, J. (2018). *Simplified and Standardized Seismic Design and Detailing for Alabama Bridges.* Auburn, Alabama: Auburn University.

Yazdani, N., Eddy, S., & Cai, C. S. (2000). Effect of Bearing Pads on Precast Prestressed Concrete Bridges. *Journal of Bridge Engineering*, 224-232.

Zahrai, S. M., & Bruneau, M. (1998). Impact of Diaphragms on Seismic Response of Straight Slab-on-Girder Steel Bridges. *Journal of Structural Engineering*, 938-947.

APPENDIX A: SAMPLE CALCULATIONS

Montgomery County Bridge Design

$Weight := 13384.793\,kip$ From model vertical base reactions

$T_{long} := 1.29533$ From analytical model 1st Modal period

$T_{tranv} := 0.67212$ From analytical model 2nd Modal period

$Length := 1273.667\,ft$ From drawings

Geological Report not provided. Assume Site Class D

$N_{worst} := 50$

$$SiteClass := \begin{bmatrix} \text{"C"} & \text{if } N_{worst} > 50 \\ \text{"D"} & \text{if } \left(15 < N_{worst}\right) \le 50 \\ \text{"F"} & \text{otherwise} \end{bmatrix} = \text{"D"}$$

Guide Table 3.4.2.1-1

$S_{D1} := .104$ From county acceleration maps

$S_{DS} := .154$ From county acceleration maps

$$SDC := \begin{bmatrix} \text{"A"} & \text{if } S_{D1} < 0.15 \\ \text{"B"} & \text{if } 0.15 \le S_{D1} < 0.30 \\ \text{"C"} & \text{if } 0.30 \le S_{D1} < 0.50 \\ \text{"D"} & \text{otherwise} \end{bmatrix} = \text{"A"}$$

Guide Table 3.5-1

$$T_s := \frac{S_{D1}}{S_{DS}} = 0.675$$

Guide EQ 3.4.1-6

$T_{star} := 1.25 \cdot T_s = 0.844$ Guide EQ 4.3.3-3

$T_0 := 0.2 \cdot T_s = 0.135$ Guide EQ 3.4.1-5

$\mu_D := 1$ Guide 4.3.3 μ.D not specified for SDC A

$A_s := 0.067$ From county acceleration maps

$$S_{a\_long} := \begin{cases} \left[\left(S_{DS} - A_s\right) \cdot \frac{T_{long}}{T_0} + A_s\right] & \text{if } T_{long} < T_0 = 0.08 \quad \text{Guide EQ 3.4.1-4} \\ S_{DS} & \text{if } T_0 < T_{long} < T_s \quad \text{Guide EQ 3.4.1-7} \\ \frac{S_{D1}}{T_{long}} & \text{otherwise} \quad \text{Guide EQ 3.4.1-8} \end{cases}$$

$$S_{a\_tranv} := \begin{cases} \left[\left(S_{DS} - A_s\right) \cdot \frac{T_{tranv}}{T_0} + A_s\right] & \text{if } T_{tranv} < T_0 = 0.154 \quad \text{Guide EQ 3.4.1-4} \\ S_{DS} & \text{if } T_0 < T_{tranv} < T_s \quad \text{Guide EQ 3.4.1-7} \\ \frac{S_{D1}}{T_{tranv}} & \text{otherwise} \quad \text{Guide EQ 3.4.1-8} \end{cases}$$

$p_{e\_long} := \frac{S_{a\_long} \cdot Weight}{Length} = 0.844 \cdot \frac{kip}{ft}$ Guide EQ C5.4.2-4

$p_{e\_tranv} := \frac{S_{a\_tranv} \cdot Weight}{Length} = 1.618 \cdot \frac{kip}{ft}$ Guide EQ C5.4.2-4

$$CapacityCheck(demand, capacity) := \begin{cases} \text{"OK"} & \text{if } demand < capacity \\ \text{"Capacity exceeded"} & \text{otherwise} \end{cases}$$

$$RequirementCheck(requirement, calculation) := \begin{cases} \text{"OK"} & \text{if } calculation < requirement \\ \text{"NOT OK"} & \text{otherwise} \end{cases}$$

Connection Design Check

Transverse Shear

Earthquake Loads

$v_{TEQ7} := -2.01kip + -35.91kip$ Transverse EQ shear in critical bearing connection at Bent 7

$v_{TEQ8} := 3.72kip + -77.58kip$ Transverse EQ shear in critical bearing connection at Bent 8

$v_{TEQ9} := 4.01kip + -59.5kip$ Transverse EQ shear in critical bearing connection at Bent 9

$v_{TEQ10} := -32.31kip + 2.59kip$ Transverse EQ shear in critical bearing connection at Abut 10

Dead Loads

$v_{TDL7} := -3.31kip$ Transverse DL shear in critical bearing connection at Bent 7

$v_{TDL8} := -1.83kip$ Transverse DL shear in critical bearing connection at Bent 8

$v_{TDL9} := -4.27kip$ Transverse DL shear in critical bearing connection at Bent 9

$v_{TDL10} := 0.93kip$ Transverse DL shear in critical bearing connection at Abut 10

Factored Loads

$v_{bent7connec} := 1.25 \cdot v_{TDL7} + v_{TEQ7} = -42.057 \cdot kip$ LRFD Table 4.3.1-1 abd 4.3.1-2

$v_{bent8connec} := 1.25 \cdot v_{TDL8} + v_{TEQ8} = -76.147 \cdot kip$

$v_{bent9connec} := 1.25 \cdot v_{TDL9} + v_{TEQ9} = -60.827 \cdot kip$

$v_{abut10connec} := 1.25 \cdot v_{TDL10} + v_{TEQ10} = -28.558 \cdot kip$

Weld Design

$F_{exx} := 70ksi$ Yield strength of weld metal

$t_{soleplate} := \frac{40}{25.4}in = 1.575 \cdot in$ Thickness of sole palte

$F_{yplate} := 36ksi$ Yield stress of sole plate

$F_{uplate} := 58ksi$ Ultimate tensile stress of sole plate

$L_{weldbent7} := 20in$ Weld length at bent 7

$L_{weldbent8} := 30in$ Weld length at bent 8

$L_{weldbent9} := 30in$ Weld length at bent 9

$L_{weldabut10} := 20in$ Weld length at abutment 10

$Number_{welds} := 2$ Number of welds for connection

$weld_{size} := \frac{5}{16}in$ Fillet weld throat size

Base Metal Tension LRFD 6.13.5.2

$\phi_y := 0.95$ Resistance factor for yielding on gross section

$\phi_u := 0.80$ Resistance factor for rupture on net section

$U := 1$ Shear lag factor for welded members in tension

$A_{plate7} := L_{weldbent7} \cdot t_{soleplate} = 31.496 \cdot in^2$

$A_{plate8} := L_{weldbent8} \cdot t_{soleplate} = 47.244 \cdot in^2$

$A_{plate9} := L_{weldbent9} \cdot t_{soleplate} = 47.244 \cdot in^2$

$A_{plate10} := L_{weldabut10} \cdot t_{soleplate} = 31.496 \cdot in^2$

$\phi R_{baserupture7} := \min\left(\phi_y \cdot F_{yplate} \cdot A_{plate7}, \phi_u \cdot F_{uplate} \cdot A_{plate7} \cdot U\right) = 1077.165 \cdot kip$

$\phi R_{baserupture8} := \min\left(\phi_y \cdot F_{yplate} \cdot A_{plate8}, \phi_u \cdot F_{uplate} \cdot A_{plate8} \cdot U\right) = 1615.748 \cdot kip$

$\phi R_{baserupture9} := \min\left(\phi_y \cdot F_{yplate} \cdot A_{plate9}, \phi_u \cdot F_{uplate} \cdot A_{plate9} \cdot U\right) = 1615.748 \cdot kip$

$\phi R_{baserupture10} := \min\left(\phi_y \cdot F_{yplate} \cdot A_{plate10}, \phi_u \cdot F_{uplate} \cdot A_{plate10} \cdot U\right) = 1077.165 \cdot kip$

Base Metal Shear LRFD 6.13.5.3

$\phi_v := 1.0$ Resistance factor for base metal shear

$\phi R_{baseshear7} := \phi_v \cdot 0.58 \cdot F_{yplate} \cdot A_{plate7} = 657.638 \cdot kip$

$\phi R_{baseshear8} := \phi_v \cdot 0.58 \cdot F_{yplate} \cdot A_{plate8} = 986.457 \cdot kip$

$\phi R_{baseshear9} := \phi_v \cdot 0.58 \cdot F_{yplate} \cdot A_{plate9} = 986.457 \cdot kip$

$\phi R_{baseshear10} := \phi_v \cdot 0.58 \cdot F_{yplate} \cdot A_{plate10} = 657.638 \cdot kip$

Weld Metal Shear Rupture LRFD 6.13.3.2.3

$\phi_{e2} := 0.80$ Resistance factor for base metal shear rupture

$R_{rShear} := 0.6 \cdot \phi_{e2} \cdot F_{exx}$ Factored Resistance LRFD 6.13.3.2.4b-1

$A_{effbent7} := .707 \cdot weld_{size} \cdot L_{weldbent7} \cdot Number_{welds} = 8.837 \cdot in^2$ Effective weld area LRFD 6.13.3.3

$A_{effbent8} := .707 \cdot weld_{size} \cdot L_{weldbent8} \cdot Number_{welds} = 13.256 \cdot in^2$

$A_{effbent9} := .707 \cdot weld_{size} \cdot L_{weldbent9} \cdot Number_{welds} = 13.256 \cdot in^2$

$A_{effabut10} := .707 \cdot weld_{size} \cdot L_{weldabut10} \cdot Number_{welds} = 8.837 \cdot in^2$

$\phi R_{weld7} := \phi_{e2} \cdot A_{effbent7} \cdot R_{rShear} = 237.552 \cdot kip$

$\phi R_{weld8} := \phi_{e2} \cdot A_{effbent8} \cdot R_{rShear} = 356.328 \cdot kip$

$\phi R_{weld9} := \phi_{e2} \cdot A_{effbent9} \cdot R_{rShear} = 356.328 \cdot kip$

$\phi R_{weld10} := \phi_{e2} \cdot A_{effabut10} \cdot R_{rShear} = 237.552 \cdot kip$

Weld Capacity

$\phi Weld_{bent7} := \min(\phi R_{baserupture7}, \phi R_{baseshear7}, \phi R_{weld7}) = 237.552 \cdot kip$

$\phi Weld_{bent8} := \min(\phi R_{baserupture8}, \phi R_{baseshear8}, \phi R_{weld8}) = 356.328 \cdot kip$

$\phi Weld_{bent9} := \min(\phi R_{baserupture9}, \phi R_{baseshear9}, \phi R_{weld9}) = 356.328 \cdot kip$

$\phi Weld_{abut10} := \min(\phi R_{baserupture10}, \phi R_{baseshear10}, \phi R_{weld10}) = 237.552 \cdot kip$

$CapacityCheck(|v_{bent7connec}|, \phi Weld_{bent7}) = "OK"$

$CapacityCheck(|v_{bent8connec}|, \phi Weld_{bent8}) = "OK"$

$CapacityCheck(|v_{bent9connec}|, \phi Weld_{bent9}) = "OK"$

$CapacityCheck(|v_{abut10connec}|, \phi Weld_{abut10}) = "OK"$

Anchor Bolt Design

Flexural Demand

$Dia := 1.5in$ Diameter of anchor bolts

$E := 29000ksi$

$slotwidth := \frac{45}{25.4} in = 1.772 \cdot in$ Width of bolt slot

$t_{soleplate} = 1.575 \cdot in$ Thickness of sole plate

$L_{anchorbent7} := 7.2in$ Length of anchor bolt at bent 7

$L_{anchorbent8} := 4.75in$ Length of anchor bolt at bent 8

$L_{anchorbent9} := 4.75in$ Length of anchor bolt at bent 9

$L_{anchorabut10} := 4.75in$ Length of anchor bolt at abutment 10

$$I_{anchor} := \frac{\pi}{4} \cdot \left(\frac{Dia}{2} \right)^4 = 0.249 \cdot in^4$$ Moment of inertia of anchor bolt

Calculate the force required to deflect the anchor bolt till it comes into contact with the sole plate.
This force creates bending moment as a cantilever element ("cant")

$$P_{bent7cant} := \frac{(slotwidth - Dia) \cdot 3 \cdot E \cdot I_{anchor}}{\left(L_{anchorbent7} - \frac{t_{soleplate}}{2} \right)^3} = 22.272 \cdot kip$$

$$P_{bent7cant} := \begin{cases} P_{bent7cant} & \text{if } P_{bent7cant} < \left| v_{bent7connec} \right| \\ \left| v_{bent7connec} \right| & \text{otherwise} \end{cases} = 22.272 \cdot kip$$

Cantilever force can't be greater than actual shear force from model

$$P_{bent8cant} := \frac{(slotwidth - Dia) \cdot 3 \cdot E \cdot I_{anchor}}{\left(L_{anchorbent8} - \frac{t_{soleplate}}{2} \right)^3} = 94.391 \cdot kip$$

$$P_{bent8cant} := \begin{cases} P_{bent8cant} & \text{if } P_{bent8cant} < \left| v_{bent8connec} \right| \\ \left| v_{bent8connec} \right| & \text{otherwise} \end{cases} = 76.147 \cdot kip$$

$$P_{bent9cant} := \frac{(slotwidth - Dia) \cdot 3 \cdot E \cdot I_{anchor}}{\left(L_{anchorbent9} - \frac{t_{soleplate}}{2} \right)^3} = 94.391 \cdot kip$$

$$P_{bent9cant} := \begin{cases} P_{bent9cant} & \text{if } P_{bent9cant} < \left|v_{bent9connec}\right| \\ \left|v_{bent9connec}\right| & \text{otherwise} \end{cases} = 60.827 \cdot kip$$

$$P_{abut10cant} := \frac{(slotwidth - Dia) \cdot 3 \cdot E \cdot I_{anchor}}{\left(L_{anchorabut10} - \frac{t_{soleplate}}{2}\right)^3} = 94.391 \cdot kip$$

$$P_{abut10cant} := \begin{cases} P_{abut10cant} & \text{if } P_{abut10cant} < \left|v_{abut10connec}\right| \\ \left|v_{abut10connec}\right| & \text{otherwise} \end{cases} = 28.558 \cdot kip$$

After the anchor bends as a cantilever element, it will contact the sole plate and behave as a fixed-fixed connection. The difference between the actual shear force and the cantilever force is the remaining force left to bend the anchor bolt as a fixed-fixed element

$$P_{bent7fixed} := \begin{cases} \left(\left|v_{bent7connec}\right| - P_{bent7cant}\right) & \text{if } \left(\left|v_{bent7connec}\right| - P_{bent7cant}\right) > 0 \\ 0 & \text{otherwise} \end{cases} = 19.785 \cdot kip$$

$$P_{bent8fixed} := \begin{cases} \left(\left|v_{bent8connec}\right| - P_{bent8cant}\right) & \text{if } \left(\left|v_{bent8connec}\right| - P_{bent8cant}\right) > 0 \\ 0 & \text{otherwise} \end{cases} = 0 \cdot kip$$

$$P_{bent9fixed} := \begin{cases} \left(\left|v_{bent9connec}\right| - P_{bent9cant}\right) & \text{if } \left(\left|v_{bent9connec}\right| - P_{bent9cant}\right) > 0 \\ 0 & \text{otherwise} \end{cases} = 0 \cdot kip$$

$$P_{abut10fixed} := \begin{cases} \left(\left|v_{abut10connec}\right| - P_{abut10cant}\right) & \text{if } \left(\left|v_{abut10connec}\right| - P_{abut10cant}\right) > 0 \\ 0 & \text{otherwise} \end{cases} = 0 \cdot kip$$

Flexural demand is the total from the cantilever and fixed-fixed bending

$$M_{bent7connec} := P_{bent7cant} \cdot \left(L_{anchorbent7} - \frac{t_{soleplate}}{2}\right) + 0.5 \cdot P_{bent7fixed} \cdot \left(L_{anchorbent7} - \frac{t_{soleplate}}{2}\right)$$

$$M_{bent7connec} = 206.261 \cdot kip \cdot in$$

$$M_{bent8connec} := P_{bent8cant}\cdot\left(L_{anchorbent8} - \frac{t_{soleplate}}{2}\right) + 0.5P_{bent8fixed}\cdot\left(L_{anchorbent8} - \frac{t_{soleplate}}{2}\right)$$

$$M_{bent8connec} = 301.742\cdot kip\cdot in$$

$$M_{bent9connec} := P_{bent9cant}\cdot\left(L_{anchorbent9} - \frac{t_{soleplate}}{2}\right) + 0.5P_{bent9fixed}\cdot\left(L_{anchorbent9} - \frac{t_{soleplate}}{2}\right)$$

$$M_{bent9connec} = 241.035\cdot kip\cdot in$$

$$M_{abut10connec} := P_{abut10cant}\cdot\left(L_{anchorabut10} - \frac{t_{soleplate}}{2}\right) + 0.5P_{abut10fixed}\cdot\left(L_{anchorabut10} - \frac{t_{solep}}{2}\right.$$

$$M_{abut10connec} = 113.162\cdot kip\cdot in$$

Flexural Strength

$F_y := 60ksi$ Yield strength of anchor bolt

$\phi_f := 1.0$ Flexural resistance factor

$A_{bolt} := \frac{\pi}{4}\cdot Dia^2 = 1.767\cdot in^2$ Area of bolt

$Z := \frac{1}{2}\cdot A_{bolt}\cdot\frac{4\cdot\frac{Dia}{2}}{3\pi}\cdot 2 = 0.562\cdot in^3$ Plastic section modulus

$S := \frac{\pi\cdot\left(\frac{Dia}{2}\right)^3}{4} = 0.331\cdot in^3$ Elastic section modulus

$N_{bolts7} := 4$ Number of bolts at bent 7

$M_{nbent7} := \min\left(F_y\cdot Z, 1.6\cdot F_y\cdot S\right)\cdot N_{bolts7} = 127.235\cdot kip\cdot in$ LRFD EQ 6.12.2.2.7-1

$\phi_f\cdot M_{nbent7} = 127.235\cdot kip\cdot in$

$N_{bolts8} := 4$

$M_{nbent8} := \min\left(F_y \cdot Z, 1.6 \cdot F_y \cdot S\right) \cdot N_{bolts8} = 127.235 \cdot kip \cdot in$

$\phi_f \cdot M_{nbent8} = 127.235 \cdot kip \cdot in$

$N_{bolts9} := 4$

$M_{nbent9} := \min\left(F_y \cdot Z, 1.6 \cdot F_y \cdot S\right) \cdot N_{bolts9} = 127.235 \cdot kip \cdot in$

$\phi_f \cdot M_{nbent9} = 127.235 \cdot kip \cdot in$

$N_{bolts10} := 2$

$M_{nabut10} := \min\left(F_y \cdot Z, 1.6 \cdot F_y \cdot S\right) \cdot N_{bolts10} = 63.617 \cdot kip \cdot in$

$\phi_f \cdot M_{nabut10} = 63.617 \cdot kip \cdot in$

$\text{CapacityCheck}\left(\left|M_{bent7connec}\right|, \phi_f \cdot M_{nbent7}\right) = \text{"Capacity exceeded"}$

$\text{CapacityCheck}\left(\left|M_{bent8connec}\right|, \phi_f \cdot M_{nbent8}\right) = \text{"Capacity exceeded"}$

$\text{CapacityCheck}\left(\left|M_{bent9connec}\right|, \phi_f \cdot M_{nbent9}\right) = \text{"Capacity exceeded"}$

$\text{CapacityCheck}\left(\left|M_{abut10connec}\right|, \phi_f \cdot M_{nabut10}\right) = \text{"Capacity exceeded"}$

Shear Strength LRFD 6.13.2.12

$F_{ub} := 60ksi$ Ultimate tensile strength of bolts

$N_{splanes} := 1$ Number of shear planes per bolt

$\phi_s := .75$ Resistance factor for shear of anchor bolts

$R_{nbent7} := .48 \cdot A_{bolt} \cdot F_{ub} \cdot N_{splanes} \cdot N_{bolts7} = 203.575 \cdot kip$

$\phi_s \cdot R_{nbent7} = 152.681 \cdot kip$

$R_{nbent8} := .48 \cdot A_{bolt} \cdot F_{ub} \cdot N_{splanes} \cdot N_{bolts8} = 203.575 \cdot kip$

$\phi_s \cdot R_{nbent8} = 152.681 \cdot kip$

$R_{nbent9} := .48 \cdot A_{bolt} \cdot F_{ub} \cdot N_{splanes} \cdot N_{bolts9} = 203.575 \cdot kip$

$\phi_s \cdot R_{nbent9} = 152.681 \cdot kip$

$R_{nabut10} := .48 \cdot A_{bolt} \cdot F_{ub} \cdot N_{splanes} \cdot N_{bolts10} = 101.788 \cdot kip$

$\phi_s \cdot R_{nabut10} = 76.341 \cdot kip$

$CapacityCheck\left(\left|v_{bent7connec}\right|, \phi_s \cdot R_{nbent7}\right) = \text{"OK"}$

$CapacityCheck\left(\left|v_{bent8connec}\right|, \phi_s \cdot R_{nbent8}\right) = \text{"OK"}$

$CapacityCheck\left(\left|v_{bent9connec}\right|, \phi_s \cdot R_{nbent9}\right) = \text{"OK"}$

$CapacityCheck\left(\left|v_{abut10connec}\right|, \phi_s \cdot R_{nabut10}\right) = \text{"OK"}$

Shear Block Design

$\phi_{shear} := 0.9$ LRFD 5.5.4.2

$\phi_{tension} := 0.9$ LRFD 5.5.4.2

$\phi_{compression} := 0.75$ LRFD 5.5.4.2

$f_{cprime} := 6.5$

$f_y := 60ksi$

Note: Because Mathcad has difficulty when units are placed under a square root, dimensions are left off of the compressive strength. Any time this variable is used, the units must be added in somewhere--usually to a constant.

$V_{bent} := 281.13kip$ Bent base shear

Assume l_v is width of bent

$l_v := 60in$ Length of shear block

$a_v := L_{anchorbent7} - \frac{t_{soleplate}}{2} = 6.413 \cdot in$

Height from surface of bent cap that shear force will be applied to Shear Block. Bent 7 was chosen as it is the longest

Assume concrete cover $d_c := 3in$

$h := a_v + d_c + 0.5in = 9.913 \cdot in$

$h := 10in$

Height of the shear block will be a_v, plus the cover, plus the diameter of the transverse reinforcement. Here it is assumed that No. 4 reinforcing will be used for the transverse reinforcement.

Shear design

This spreadsheet is set up for an iterative design process. The width of the shear block (w), the shear reinforcement (A_v), and the spacing of transverse reinforcement (s) will be the three changing variables until all of the design checks are met.

Estimate $w := 78in$

Full width of the shear block. This can be estimated by the distance between adjacent girder sole plates minus a gap between the sole plate and the shear block determined by the designer.

$c := 0.4ksi$ LRFD 5.8.4.3

$\mu := 1.4$ LRFD 5.8.4.3

$A_{cv} := w \cdot l_v = 4680 \cdot in^2$

$$A_{vf.min} := \frac{0.05 \frac{kip}{in^2} \cdot A_{cv}}{f_y} = 3.9 \cdot in^2$$ LRFD 5.8.4.4

$\frac{kip}{in^2}$ applied for dimensional consistency

$V_n := c \cdot A_{cv} + \mu \cdot A_{vf.min} \cdot f_y = 2199.6 \cdot kip$ LRFD 5.8.4.1-3

$K_1 := .25$ LRFD 5.8.4.3

$K_2 := 1.5ksi$ LRFD 5.8.4.3

$V_{nmax1} := K_1 \cdot f_{cprime} \cdot A_{cv} \cdot 1ksi = 7605 \cdot kip$ LRFD 5.8.4.1-4

$V_{nmax2} := K_2 \cdot A_{cv} = 7020 \cdot kip$ LRFD 5.8.4.1-5

$\phi V_n := \min\left(\phi_{shear} \cdot V_n, V_{nmax1}, V_{nmax2}\right) = 1979.64 \cdot kip$

$\text{CapacityCheck}\left(V_{bent}, \phi V_n\right) = \text{"OK"}$

Longitudinal Shear

Earthquake Loads

$v_{LEQ7} := 14.2kip + -.99kip$ Longitudinal EQ shear in critical bearing connection at Bent 7

$v_{LEQ8} := 29.65kip + .16kip$ Longitudinal EQ shear in critical bearing connection at Bent 8

$v_{LEQ9} := 27.65kip + 3.74kip$ Longitudinal EQ shear in critical bearing connection at Bent 9

$v_{LEQ10} := 39.56kip + 3.6kip$ Longitudinal EQ shear in critical bearing connection at Abut 10

Dead Loads

$v_{LDL7} := -.38kip$ Longitudinal DL shear in critical bearing connection at Bent 7

$v_{LDL8} := 1.13kip$ Longitudinal DL shear in critical bearing connection at Bent 8

$v_{LDL9} := -.37kip$ Longitudinal DL shear in critical bearing connection at Bent 9

$v_{LDL10} := 4.85kip$ Longitudinal DL shear in critical bearing connection at Abut 10

Factored Loads:

$v_{Lbent7connec} := 1.25 \cdot v_{LDL7} + v_{LEQ7} = 12.735 \cdot kip$

$v_{Lbent8connec} := 1.25 \cdot v_{LDL8} + v_{LEQ8} = 31.223 \cdot kip$

$v_{Lbent9connec} := 1.25 \cdot v_{LDL9} + v_{LEQ9} = 30.927 \cdot kip$

$v_{Labut10connec} := 1.25 \cdot v_{LDL10} + v_{LEQ10} = 49.223 \cdot kip$

Weld Strength

$\phi Weld_{bent7} = 237.552 \cdot kip$ Weld strength is same as above

$\phi Weld_{bent8} = 356.328 \cdot kip$

$\phi Weld_{bent9} = 356.328 \cdot kip$

$\phi Weld_{abut10} = 237.552 \cdot kip$

$CapacityCheck\left(\left|v_{Lbent7connec}\right|, \phi Weld_{bent7}\right) = \text{"OK"}$

$CapacityCheck\left(\left|v_{Lbent8connec}\right|, \phi Weld_{bent8}\right) = \text{"OK"}$

$CapacityCheck\left(\left|v_{Lbent9connec}\right|, \phi Weld_{bent9}\right) = \text{"OK"}$

$CapacityCheck\left(\left|v_{Labut10connec}\right|, \phi Weld_{abut10}\right) = \text{"OK"}$

End Diaphragm Design

$\phi_w := 0.80$ Tension, fracture on the net section

$\phi_y := 0.95$ Tension, yielding in gross section LRFD 6.5.4.2

$\phi_{bs} := 0.80$ Block shear failure

$\phi_c := 0.95$ Axial compression

$E := 29000ksi$ $F_y := 36ksi$ $F_u := 58ksi$ $G := .385 \cdot E = 11165 \cdot ksi$

Top Chord C15x40

$MaxComp := .998kip$

$MaxTen := 1.06kip$

$L_b := 8.6ft$

$A_g := 11.8in^2$ $r_x := 5.43in$ $r_y := 0.883in$ $J := 1.45in^4$ $I_x := 348in^4$

$C_w := 410in^6$ $H := .927$ $r_0 := 5.71in$ $I_y := 9.17in^4$ $t_w := 0.52in$

Tension Member Design

Check slenderness ratio

$slenderness_{limit} := 140$ LRFD 6.8.4

$$slenderness_{ratio} := \frac{L_b}{r_x} = 19.006$$

$RequirementCheck(slenderness_{limit}, slenderness_{ratio}) = "OK"$

Yielding on gross section

$P_{r1} := \phi_y \cdot F_y \cdot A_g = 403.56 \cdot kip$ LRFD EQ 6.8.2.1-1

Fracture on net section

$R_p := 0.9$ Assume holes are punched

$U := 1 - \frac{.5}{8}$ Shear lag factor

$Dia_{hole} := 1in$

$Num_{holes} := 4$

$A_n := A_g - \left(Dia_{hole} + \frac{1}{16}in\right) \cdot t_w \cdot Num_{holes} = 9.59 \cdot in^2$

$P_{r2} := \phi_u \cdot F_u \cdot A_n \cdot R_p \cdot U = 375.449 \cdot kip$ LRFD EQ 6.8.2.1-2

$P_r := \min\left(P_{r1}, P_{r2}\right) = 375.449 \cdot kip$

Block shear LRFD 6.13.4

$A_{tn} := 4in \cdot t_w = 2.08 \cdot in^2$

$A_{vg} := 8in \cdot t_w = 4.16 \cdot in^2$

$A_{vn} := A_{vg} - \left(Dia_{hole} + \frac{1}{16}in\right) \cdot t_w$

$U_{bs} := 1.0$

$R_r := \min\left[\phi_{bs} \cdot R_p \cdot \left(.58 \cdot F_u \cdot A_{vn} + U_{bs} \cdot F_u \cdot A_{tn}\right), \phi_{bs} \cdot R_p \cdot \left(.58 \cdot F_y \cdot A_{vg} + U_{bs} \cdot F_u \cdot A_{tn}\right)\right] = 149.401 \cdot kip$

$TopChordCapacity := \min\left(P_r, R_r\right) = 149.401 \cdot kip$

$CapacityCheck(MaxTen, TopChordCapacity) = "OK"$

Compression Member Design

Check slenderness

$slenderness_{limit} := 120$ LRFD 6.9.3

$slenderness_{ratio} := \frac{L_b}{r_y} = 116.874$

$RequirementCheck\left(slenderness_{limit}, slenderness_{ratio}\right) = "OK"$

$k := 1.49$

$b_f := 3.52in$ $t_f := 0.65in$

$slenderness_{ratio} := \frac{b_f}{t_f} = 5.415$ LRFD 6.9.4.2

$slenderness_{limit} := k \cdot \sqrt{\frac{E}{F_y}} = 42.29$

$RequirementCheck(slenderness_{limit}, slenderness_{ratio}) = "OK"$ $Q := 1.0$

Calculate Capacity

$P_{ey} := \frac{\pi^2 \cdot E}{\frac{L_b}{r_y}} \cdot A_g = 28897.532 \cdot kip$ LRFD 6.9.4.1.2-1

$P_{ez} := \left(\frac{\pi^2 \cdot E \cdot C_w}{L_b^2} + G \cdot J \right) \cdot \frac{1}{r_0^2} = 834.488 \cdot kip$ LRFD 6.9.4.1.3-5

$P_{e.elastic} := P_{ey}$

$P_{e.FTB} := \frac{(P_{ey} + P_{ez})}{2 \cdot H} \cdot \left[1 - \sqrt{1 - \frac{4 \cdot P_{ey} \cdot P_{ez} \cdot H}{(P_{ey} + P_{ez})^2}} \right] = 832.685 \cdot kip$ LRFD 6.9.4.1.3-2

$P_e := \min(P_{e.elastic}, P_{e.FTB}) = 832.685 \cdot kip$

$P_o := Q \cdot F_y \cdot A_g = 424.8 \cdot kip$ LRFD 6.9.4.1.1

$P_n := \begin{cases} (.877 \cdot P_e) & \text{if } \frac{P_e}{P_o} < 0.44 \quad = 343.124 \cdot kip \\ \left[\left(.658^{\frac{P_o}{P_e}} \right) \cdot P_o \right] & \text{otherwise} \end{cases}$ LRFD 6.9.4.1.1-2 / LRFD 6.9.4.1.1-1

$\phi_c \cdot P_n = 325.968 \cdot kip$

$CapacityCheck(MaxComp, \phi_c \cdot P_n) = "OK"$

Bot Chord L6x6x1/2

$MaxComp := 3.38kip$

$MaxTen := 3.55kip$

$L_b := 8.6ft$

$A_g := 5.77in^2$ $r_x := 1.86in$ $r_y := 1.86in$ $J := .501in^4$ $I_x := 19.9in^4$

$C_w := 1.32in^6$ $r_0 := 3.31in$ $I_y := 19.9in^4$

Tension Member Design

Check slenderness ratio

$slenderness_{limit} := 140$ LRFD 6.8.4

$slenderness_{ratio} := \frac{L_b}{r_x} = 55.484$

$RequirementCheck(slenderness_{limit}, slenderness_{ratio}) = "OK"$

Yielding on gross section

$P_{r1} := \phi_y \cdot F_y \cdot A_g = 197.334 \cdot kip$ LRFD EQ 6.8.2.1-1

Fracture on net section

$R_p := 1.0$ No holes

$U := 0.60$ Shear lag factor

$A_n := A_g$ No area taken out of gross section because x-section is welded

$P_{r2} := \phi_u \cdot F_u \cdot A_n \cdot R_p \cdot U = 160.637 \cdot kip$ LRFD EQ 6.8.2.1-2

$P_r := \min(P_{r1}, P_{r2}) = 160.637 \cdot kip$

Block shear LRFD 6.13.4

$A_{tn} := 2 \cdot 6in \cdot \frac{5}{16}in = 3.75 \cdot in^2$

$A_{vg} := 6in \cdot \frac{5}{16}in = 1.875 \cdot in^2$

$A_{vn} := A_{vg}$

$U_{bs} := 1.0$

$R_r := \min\left[\phi_{bs} \cdot R_p \cdot \left(.58 \cdot F_u \cdot A_{vn} + U_{bs} \cdot F_u \cdot A_{tn}\right), \phi_{bs} \cdot R_p \cdot \left(.58 \cdot F_y \cdot A_{vg} + U_{bs} \cdot F_u \cdot A_{tn}\right)\right] = 205.32 \cdot kip$

$TopChordCapacity := \min\left(P_r, R_r\right) = 160.637 \cdot kip$

$CapacityCheck(MaxTen, TopChordCapacity) = "OK"$

Compression Member Design

Check slenderness

$slenderness_{limit} := 120$ LRFD 6.9.3

$slenderness_{ratio} := \frac{L_b}{r_y} = 55.484$

$RequirementCheck\left(slenderness_{limit}, slenderness_{ratio}\right) = "OK"$

$k := .45$

$b_f := 6in$ $t_f := .50in$

$slenderness_{ratio} := \frac{b_f}{t_f} = 12$ LRFD 6.9.4.2

$slenderness_{limit} := k \cdot \sqrt{\frac{E}{F_y}} = 12.772$

$RequirementCheck\left(slenderness_{limit}, slenderness_{ratio}\right) = "OK"$

USE Q=1.0 if "OK", Otherwise use below EQ for Q

$$Q := \begin{cases} \left(1.34 - .76 \cdot \frac{b_f}{t_f} \cdot \sqrt{\frac{F_y}{E}}\right) & \text{if } .45\sqrt{\frac{E}{F_y}} < \frac{b_f}{t_f} \le .91\sqrt{\frac{E}{F_y}} = 1 \\ \frac{.53 \cdot E}{F_y \cdot \left(\frac{b_f}{t_f}\right)^2} & \text{if } \frac{b_f}{t_f} > .91 \cdot \sqrt{\frac{E}{F_y}} \\ 1.0 & \text{otherwise} \end{cases}$$

LRFD EQ 6.9.4.2.2-5

LRFD EQ 6.9.4.2.2-6

Calculate $(KL/r)_{eff}$

$$EffSlendernessRatio := \begin{cases} \left(32 + 1.25 \cdot \frac{L_b}{r_x}\right) & \text{if } \frac{L_b}{r_x} > 80 \quad = 113.613 \\ \left(72 + .75 \cdot \frac{L_b}{r_x}\right) & \text{otherwise} \end{cases}$$

LRFD EQ 6.9.4.4-2

LRFD EQ 6.9.4.4-1

Calculate Capacity

$$P_e := \frac{\pi^2 \cdot E}{EffSlendernessRatio} \cdot A_g = 14536.033 \cdot kip$$

LRFD 6.9.4.1.2-1

$$P_o := Q \cdot F_y \cdot A_g = 207.72 \cdot kip$$

LRFD 6.9.4.1.1

$$P_n := \begin{cases} (.877 \cdot P_e) & \text{if } \frac{P_e}{P_o} < 0.44 \quad = 206.481 \cdot kip \\ \left[\left(.658^{\frac{P_o}{P_e}}\right) \cdot P_o\right] & \text{otherwise} \end{cases}$$

LRFD 6.9.4.1.1-2

LRFD 6.9.4.1.1-1

$\phi_c \cdot P_n = 196.157 \cdot kip$

$CapacityCheck(MaxComp, \phi_c \cdot P_n) = "OK"$

Diagonal L6x6x1/2

$MaxComp := 13.41 kip$

$MaxTen := 13.49 kip$

$L_b := 11.1 ft$

$A_g := 5.77in^2$ $r_x := 1.86in$ $r_y := 1.86in$ $J := .501in^4$ $I_x := 19.9in^4$

$C_w := 1.32in^6$ $r_0 := 3.31in$ $I_y := 19.9in^4$

Tension Member Design

Check slenderness ratio

$slenderness_{limit} := 140$ LRFD 6.8.4

$slenderness_{ratio} := \frac{L_b}{r_x} = 71.613$

$RequirementCheck(slenderness_{limit}, slenderness_{ratio}) = "OK"$

Yielding on gross section

$P_{r1} := \phi_y \cdot F_y \cdot A_g = 197.334 \cdot kip$ LRFD EQ 6.8.2.1-1

Fracture on net section

$R_p := 1.0$ No holes

$U := 0.60$ Shear lag factor

$A_n := A_g$ No area taken out of gross section because x-section is welded

$P_{r2} := \phi_u \cdot F_u \cdot A_n \cdot R_p \cdot U = 160.637 \cdot kip$ LRFD EQ 6.8.2.1-2

$P_r := \min(P_{r1}, P_{r2}) = 160.637 \cdot kip$

Block shear LRFD 6.13.4

$A_{tn} := 2 \cdot 6in \cdot \frac{5}{16}in = 3.75 \cdot in^2$

$A_{vg} := 6in \cdot \frac{5}{16}in = 1.875 \cdot in^2$

$A_{vn} := A_{vg}$

$U_{bs} := 1.0$

$R_r := \min\left[\phi_{bs}\cdot R_p\cdot\left(.58\cdot F_u\cdot A_{vn} + U_{bs}\cdot F_u\cdot A_{tn}\right), \phi_{bs}\cdot R_p\cdot\left(.58\cdot F_y\cdot A_{vg} + U_{bs}\cdot F_u\cdot A_{tn}\right)\right] = 205.32\cdot kip$

$TopChordCapacity := \min\left(P_r, R_r\right) = 160.637\cdot kip$

$CapacityCheck(MaxTen, TopChordCapacity) = "OK"$

Compression Member Design

Check slenderness

$slenderness_{limit} := 120$ LRFD 6.9.3

$slenderness_{ratio} := \frac{L_b}{r_y} = 71.613$

$RequirementCheck\left(slenderness_{limit}, slenderness_{ratio}\right) = "OK"$

$k := .45$

$b_f := 6in$ $t_f := .50in$

$slenderness_{ratio} := \frac{b_f}{t_f} = 12$ LRFD 6.9.4.2

$slenderness_{limit} := k\cdot\sqrt{\frac{E}{F_y}} = 12.772$

$RequirementCheck\left(slenderness_{limit}, slenderness_{ratio}\right) = "OK"$

USE Q=1.0 if "OK", Otherwise use below EQ for Q

$$Q := \begin{cases} \left(1.34 - .76\cdot\frac{b_f}{t_f}\cdot\sqrt{\frac{F_y}{E}}\right) & \text{if } .45\sqrt{\frac{E}{F_y}} < \frac{b_f}{t_f} \le .91\sqrt{\frac{E}{F_y}} = 1 \quad \text{LRFD EQ 6.9.4.2.2-5} \\ \frac{.53\cdot E}{F_y\cdot\left(\frac{b_f}{t_f}\right)^2} & \text{if } \frac{b_f}{t_f} > .91\cdot\sqrt{\frac{E}{F_y}} \quad \text{LRFD EQ 6.9.4.2.2-6} \\ 1.0 & \text{otherwise} \end{cases}$$

Calculate $(KL/r)_{eff}$

$$EffSlendernessRatio := \begin{cases} \left(32 + 1.25 \cdot \frac{L_b}{r_x}\right) & \text{if } \frac{L_b}{r_x} > 80 \\ \left(72 + .75 \cdot \frac{L_b}{r_x}\right) & \text{otherwise} \end{cases} = 125.71$$

LRFD EQ 6.9.4.4-2

LRFD EQ 6.9.4.4-1

Calculate Capacity

$$P_o := \frac{\pi^2 \cdot E}{EffSlendernessRatio} \cdot A_g = 13137.261 \cdot kip$$

LRFD 6.9.4.1.2-1

$$P_o := Q \cdot F_y \cdot A_g = 207.72 \cdot kip$$

LRFD 6.9.4.1.1

$$P_n := \begin{cases} \left(.877 \cdot P_e\right) & \text{if } \frac{P_e}{P_o} < 0.44 \\ \left[\left(\frac{P_o}{P_e}\right)^{.658}\right] \cdot P_o & \text{otherwise} \end{cases} = 206.35 \cdot kip$$

LRFD 6.9.4.1.1-2

LRFD 6.9.4.1.1-1

$\phi_c \cdot P_n = 196.032 \cdot kip$

$CapacityCheck\left(MaxComp, \phi_c \cdot P_n\right) = \text{"OK"}$